


Biogenic amine neurotransmitters promote eicosanoid production and protein homeostasis

Kishore K Joshi¹, Tarmie L Matlack¹, Stephanie Pyonteck¹, Mehul Vora¹ , Ralph Menzel² & Christopher Rongo^{1,*} 

Abstract

Metazoans use protein homeostasis (proteostasis) pathways to respond to adverse physiological conditions, changing environment, and aging. The nervous system regulates proteostasis in different tissues, but the mechanism is not understood. Here, we show that *Caenorhabditis elegans* employs biogenic amine neurotransmitters to regulate ubiquitin proteasome system (UPS) proteostasis in epithelia. Mutants for biogenic amine synthesis show decreased poly-ubiquitination and turnover of a GFP-based UPS substrate. Using RNA-seq and mass spectrometry, we found that biogenic amines promote eicosanoid production from polyunsaturated fats (PUFAs) by regulating expression of cytochrome P450 monooxygenases. Mutants for one of these P450s share the same UPS phenotype observed in biogenic amine mutants. The production of *n*-6 eicosanoids is required for UPS substrate turnover, whereas accumulation of *n*-6 eicosanoids accelerates turnover. Our results suggest that sensory neurons secrete biogenic amines to modulate lipid signaling, which in turn activates stress response pathways to maintain UPS proteostasis.

Keywords dopamine; eicosanoid; protein homeostasis; serotonin; ubiquitin

Subject Categories Metabolism; Neuroscience; Post-translational Modifications & Proteolysis

DOI 10.15252/embr.202051063 | Received 9 June 2020 | Revised 7 December 2020 | Accepted 15 December 2020 | Published online 20 January 2021

EMBO Reports (2021) 22: e51063

Introduction

Cells employ multiple signaling pathways and mechanisms for maintaining the folded state and function of their proteins, a process termed protein homeostasis (proteostasis) (Balch *et al.*, 2008; Hipp *et al.*, 2019). Challenges to proteostasis can come from changes in the environment (e.g., extreme temperature), altered internal physiology (e.g., reactive oxygen species or ROS from mitochondrial dysfunction), and physiologically associated decline due to aging (Shore & Ruvkun, 2013; Warnatsch *et al.*, 2013). Proteostasis response pathways offset these challenges by either restoring proper

protein folding or removing unfolded or damaged proteins from cells. The failure to maintain proteostasis in the face of such challenges results in physiological decline from the accumulation of oxidized and/or unfolded proteins.

One of the key pathways that removes damaged and unfolded proteins is the ubiquitin proteasome system (UPS), which covalently attaches chains of the small protein ubiquitin to lysine side chains of protein substrates (Ciechanover & Stanhill, 2014). E3-type ubiquitin ligases either specifically recognize protein substrates or recognize unfolded proteins with the help of chaperone adapters, attaching single ubiquitin protein moieties (a process called mono-ubiquitination) to these substrates (Zheng & Shabek, 2017). E4-type ubiquitin ligases recognize mono-ubiquitinated proteins and attach additional ubiquitin molecules to the initial ubiquitin, resulting in poly-ubiquitin chains (Hoppe, 2005). Poly-ubiquitinated substrates are then degraded by proteolysis via the 26S proteasome (Bard *et al.*, 2018). Aggregation-prone poly-ubiquitinated proteins are sometimes resistant to proteasomal degradation and must be recognized and removed by additional proteostasis response pathways, including the autophagy pathway (Kirkin *et al.*, 2009; Ryno *et al.*, 2013; Ciechanover & Kwon, 2015; Cortes & La Spada, 2015; Lim & Yue, 2015). It is unclear how these different pathways are coordinated or how some substrates are preferred by one pathway over another (Kocaturk & Gozuacik, 2018).

Multicellularity affords organisms the ability to employ different proteostasis pathways depending on the type of tissue or the particular proteostasis challenge. In metazoans, the nervous system coordinates physiology, including proteostasis, in multiple tissues by releasing humoral signals throughout the body (Balch *et al.*, 2008; van Oosten-Hawle & Morimoto, 2014; O'Brien & van Oosten-Hawle, 2016). Biogenic amines—a family of neurotransmitters formed from the decarboxylation of amino acids—can act as such humoral signals when released into the body from neurosecretory cells or even non-neuronal cells (Zeng *et al.*, 2007; Ng *et al.*, 2015; Morgese & Trabace, 2019). In the nematode *Caenorhabditis elegans*, thermosensory neurons release the biogenic amine neurotransmitter serotonin, which is then able to activate the expression of heat-shock proteins (HSPs) in distal tissues (Prahlaad *et al.*, 2008; Tatum *et al.*, 2015). Similarly, octopaminergic sensory neurons modulate

¹ Department of Genetics, The Waksman Institute, Rutgers The State University of New Jersey, Piscataway, NJ, USA

² Institute of Biology and Ecology, Humboldt University Berlin, Berlin, Germany

*Corresponding author. Tel: +1 848 445 0955; Fax: +1 732 445 5735; E-mail: rongo@waksman.rutgers.edu

the unfolded protein response (UPR) in distal tissues (Sun *et al*, 2011; Sun *et al*, 2012). It is unclear whether biogenic amines directly mediate their effects on target tissues or act through additional signaling intermediates to modulate proteostasis.

We previously identified novel regulators of ubiquitin-mediated proteostasis in *C. elegans* by using Ub^{G76V}-GFP, a ubiquitin fusion degradation (UFD) substrate expressed from a transgene, to monitor UPS activity (Liu *et al*, 2011; Joshi *et al*, 2016). Ub^{G76V}-GFP contains a non-cleavable ubiquitin placed amino-terminal to GFP (Liu *et al*, 2011; Segref *et al*, 2011), thereby mimicking a mono-ubiquitinated protein. E3- and E4-type ubiquitin ligases in the UFD complex attach additional ubiquitins to the K48 residue of Ub^{G76V}-GFP, resulting in poly-ubiquitination and proteasomal degradation of this reporter (Butt *et al*, 1988; Johnson *et al*, 1995; Dantuma *et al*, 2000). Ub^{G76V}-GFP degradation was previously monitored in *C. elegans* intestinal or hypodermal epithelia when this UFD substrate was expressed from either the *sur-5* or *col-19* promoter, respectively (Liu *et al*, 2011; Segref *et al*, 2011). Using this reporter, we found that the biogenic amine dopamine non-autonomously promotes UPS activity in intestinal and hypodermal epithelia in *C. elegans* (Joshi *et al*, 2016). Whether *C. elegans* employs other biogenic amines to regulate the UPS is unknown.

Caenorhabditis elegans has four biogenic amine neurotransmitters: serotonin (5-HT), dopamine (DA), octopamine (OA), and tyramine (TA) (Chase & Koelle, 2007). The *tph-1* gene encodes the *C. elegans* tryptophan hydroxylase, the key enzyme for 5-HT biosynthesis from tryptophan (Sze *et al*, 2000). The *cat-2* gene encodes the *C. elegans* tyrosine hydroxylase, which catalyzes the rate-limiting step in DA synthesis from tyrosine (Lints & Emmons, 1999). The biogenic amines TA and OA are also synthesized from tyrosine but along a different biochemical pathway (Alkema *et al*, 2005). OA is made from TA, and mutants for the *tth-1* tyramine beta hydroxylase fail to produce OA, whereas mutants for *tdc-1* tyrosine decarboxylase produce neither OA nor TA. Although TA and OA are synthesized along the same pathway, they have independent functions, and all four neurotransmitters modulate multiple neural circuits involved in locomotion, egg laying, response to food, or feeding behaviors in *C. elegans* (Chase & Koelle, 2007). The full scope of their signaling is not known.

Here, we used the Ub^{G76V}-GFP reporter to examine UPS activity in mutants that fail to synthesize the different biogenic amines in *C. elegans*. We found that the biogenic amine neurotransmitters DA, 5-HT, and TA modulate Ub^{G76V}-GFP turnover in epithelia, as hypodermal epithelia in mutants lacking DA, 5-HT, or TA show increased stability of the otherwise unstable Ub^{G76V}-GFP reporter protein. Using RNA-seq, we determined the expression profile of biogenic amine mutants and found that biogenic amine signaling promotes the expression of a specific subclass of cytochrome P450 monooxygenases (P450s) involved in the production of eicosanoids from poly-unsaturated fatty acids (PUFAs). Mutants for one of these regulated P450s, *cyp-34A4*, showed stabilized Ub^{G76V}-GFP, similar to the phenotype observed in biogenic amine mutants. Consistent with our expression profile analysis, we found that biogenic amine mutants have depressed levels of eicosanoids. As eicosanoids are derived from *n*-3 or *n*-6 long-chain PUFAs, we examined mutants impaired for PUFA synthesis and found that *n*-6 lipids are necessary and sufficient to promote Ub^{G76V}-GFP turnover. Our results suggest that neurons use biogenic amine

neurotransmitters as neurohormonal signals to modulate eicosanoid production from PUFAs. These eicosanoids in turn regulate ubiquitin-mediated proteostasis response pathways in non-neuronal tissues.

Results

The Ub^{G76V}-GFP transgene reports UPS activity

We sought to examine ubiquitin-mediated proteostasis in the hypodermis—the epithelial layer surrounding the nematode body cavity and responsible for body growth and synthesis of the outer barrier of the collagenous cuticle. The *odIs77* integrated transgene expresses both the chimeric Ub^{G76V}-GFP protein and mRFP in the hypodermis from the *col-19* promoter (Liu *et al*, 2011). The levels of Ub^{G76V}-GFP, which is a UPS substrate, can be compared to the levels of mRFP, which remains stable (Fig 1A). The mRFP allows researchers to quickly rule out changes in transgene expression versus changes in Ub^{G76V}-GFP protein degradation. While mRFP protein remains stable, the Ub^{G76V}-GFP protein is rapidly degraded as nematodes move from the first day of adulthood (Fig 1B and D; L4 + 24 h) into the second day of adulthood (Fig 1C and E; L4 + 48 h), and this turnover is largely prevented when either the UFD complex or the proteasome is inhibited (Joshi *et al*, 2016). The ratio of Ub^{G76V}-GFP to mRFP levels inversely reflects UPS activity; thus, hypodermal UPS activity increases significantly as nematodes enter day 2 of adulthood, a period of peak fecundity.

We revalidated our transgenic reporter by examining transgenic animals impaired for UPS activity. Ub^{G76V}-GFP is poly-ubiquitinated by the UFD complex and degraded by the 26S proteasome (Liu *et al*, 2011; Segref *et al*, 2011; Joshi *et al*, 2016). Eggs harboring the *odIs77* transgene were hatched on bacterial lawns expressing RNAi constructs for either the UFD complex subunit *ufd-1*, the proteasome complex core particle subunit *pbs-5*, or an empty vector as control. Ub^{G76V}-GFP levels were elevated relative to control in the *ufd-1* and *pbs-5* RNAi knockdown experiments by both day 1 and day 2 adulthood (Fig 1J and Appendix Fig S1), consistent with UPS-mediated turnover of this chimeric reporter protein. We did not detect any significant impact of the *odIs77* transgene, which expresses Ub^{G76V}-GFP, on development or behavior (Appendix Fig S1).

We also directly examined proteasome activity by generating lysates from the animals and incubating them with the fluorescent chymotryptic substrate Suc-Leu-Leu-Val-Tyr-AMC in the presence or absence of the proteasome inhibitor epoxomicin, as previously described (Vilchez *et al*, 2012; Joshi *et al*, 2016). Knockdown of the proteasome subunit *pbs-5* resulted in diminished chymotrypsin-like proteasome activity relative to empty vector control (Fig 1K). Knockdown of *ufd-1*, a gene involved in poly-ubiquitination but not proteasome catalytic activity, did not diminish chymotrypsin-like proteasome activity, as expected (Fig 1K). The *odIs77* transgene itself did not significantly impact proteasome activity (Appendix Fig S2). These results confirm that the increased levels of the Ub^{G76V}-GFP chimeric reporter can reflect either decreases in UFD activity/capacity (and thus poly-ubiquitination) or proteasome activity/capacity. In addition, we examined Ub^{G76V}-GFP levels in established regulators of proteostasis (Appendix Fig S3), including

daf-16, *hsf-1*, *skn-1*, and *pqm-1*, and found turnover depressed in these mutants, supporting the use of the *odIs77* transgene as a sensitive reporter for changes in proteostasis (Ben-Zvi et al, 2009; Steinbaugh et al, 2015; O'Brien et al, 2018).

The transcription factor SKN-1, which is part of the oxidative stress response and homologous to human Nrf2, directly promotes the expression of proteasome subunit genes (An & Blackwell, 2003; Li et al, 2011; Niu et al, 2011; Keith et al, 2016). We examined Ub^{G76V}-GFP levels in *skn-1(zj15)*, a fertile hypomorphic allele, and *skn-1(tm3411)*, a null deletion allele that results in sterile animals (Ruf et al, 2013; Tang et al, 2015). Ub^{G76V}-GFP was present at high levels in *skn-1(zj15)* in day 1 (L4 + 24 h) adults (Fig 1F, H and L and Appendix Fig S1) and remained elevated and stable in day 2 (L4 + 48 h) and day 3 (L4 + 72 h) adults relative to wild type (Fig 1G, I and L). Ub^{G76V}-GFP was similarly stable in *skn-1(tm3411)* null mutants (Fig 1L). As *skn-1(zj15)* animals are fertile and do not require a balancer chromosome, we were able to collect large numbers of synchronized animals to measure proteasome activity. Mutants for *skn-1(zj15)* showed about a 30% decrease in chymotrypsin-like proteasome activity relative to wild type in both day 1 and day 2 adults (Fig 1M and Appendix Fig S2), consistent with the decreased levels of proteasome subunit expression (Li et al, 2011; Niu et al, 2011; Keith et al, 2016) and stabilized UPS reporter (Fig 1L) observed in mutants. Thus, in addition to providing a feedback loop to activate proteasome expression during proteotoxic stress, SKN-1 maintains baseline UPS activity.

Biogenic amine signaling modulates protein turnover

In a prior RNAi genetic screen, we found that knockdown of dopamine receptors resulted in the stabilization of the Ub^{G76V}-GFP hypodermal UPS reporter (Joshi et al, 2016). We reasoned that other biogenic amine neurotransmitters besides dopamine might regulate UPS activity. In order to test each biogenic amine for such a role, we examined mutants for specific biosynthetic enzymes (Fig 2A). We introduced the *odIs77* transgene into *cat-2(e1112)* mutants, which have a nonsense mutation in *cat-2* and fail to synthesize DA, *tph-1(mg280)* mutants, which harbor a deletion of *tph-1* sequences and fail to synthesize 5-HT, *tdc-1(ok914)* mutants, which contain a deletion of *tdc-1* sequences and fail to synthesize TA and OA, and *tbh-1(ok1196)* mutants, which harbor a deletion of *tbh-1* sequences and fail to synthesize OA (Sulston et al, 1975; Lints & Emmons, 1999; Sze et al, 2000; Alkema et al, 2005). In addition to qualitatively assessing fluorescence photomicrographs (Fig 2C–F; green and red channels merged), we quantified Ub^{G76V}-GFP and mRFP levels for each genotype (Fig 2B and K, and Appendix Fig S4). Ub^{G76V}-GFP levels in *cat-2*, *tph-1*, and *tdc-1* mutants were 30–50% higher than those in wild type in day 1 (L4 + 24 h) adults and remained higher throughout our time course analysis (Fig 2B–F). We observed no difference between *tbh-1* mutants and wild type, suggesting that OA is not required to regulate Ub^{G76V}-GFP turnover (Fig 2K).

Several additional experiments supported our conclusion that biogenic amines regulate UPS activity in the hypodermis. Investigation of additional alleles of each gene at day 2 (L4 + 48 h) was consistent and confirmed the above findings (Fig 2K). To confirm whether any observed regulation of Ub^{G76V}-GFP occurs at the level of protein stability rather than transcription, we quantified Ub^{G76V}-GFP and mRFP mRNA levels and detected no change between the

different genotypes (Appendix Fig S5), consistent with a post-transcriptional explanation for the observed differences in protein levels. We did not detect a change in developmental timing that could alternatively explain the slowed capacity for Ub^{G76V}-GFP turnover (Appendix Fig S5). Finally, the UPS phenotype for the *cat-2* and *tph-1* mutants could be rescued by supplementing their growth media with exogenous DA and 5-HT, respectively, and wild-type animals supplemented with 5-HT showed accelerated Ub^{G76V}-GFP turnover (Fig EV1). Our results indicate that UPS activity is decreased in mutants that fail to synthesize the biogenic amines DA, 5-HT, and TA, but not in mutants that fail to synthesize only OA, and that supplemental levels of 5-HT can increase activity.

Although mRFP protein levels remain unchanged in all of the biogenic amine mutants, we noticed that the protein accumulated in aggregated puncta throughout the hypodermis in day 2 (L4 + 48 h) animals (Fig 2G and H). Like most derivatives of DsRed, the monomeric RFP can aggregate in cells (Yanushevich et al, 2002; Snapp, 2005; Snaith et al, 2010). We reasoned that the change in mRFP aggregation from day 1 adults to day 2 adults might reflect the same change in proteostasis that augments Ub^{G76V}-GFP turnover. Indeed, *tph-1(mg280)* and *skn-1(zj15)* mutants showed a decrease in the number of visible mRFP aggregates (puncta) in day 1 and day 2 adults (Fig EV1). Mutants for *cat-2(e1112)* had a similar number of mRFP aggregates as wild type at day 1, but did not accumulate as many aggregates by day 2 (Figs 2I and J, and EV1). Our results suggest that in addition to promoting UPS activity, biogenic amine signaling is required for the hypodermis to sequester aggregation-prone proteins into large punctate structures.

We also examined mutants that impair signaling of more than one biogenic amine. BAS-1 encodes an aromatic amino acid decarboxylase required for the synthesis of both DA and 5-HT, CAT-1 encodes a monoamine transporter required for loading synaptic vesicles with all biogenic amines, and CAT-4 encodes a GTP cyclohydrolase required for the synthesis of multiple small compounds including DA and 5-HT (Sulston et al, 1975; Loer & Kenyon, 1993; Duerr et al, 1999; Hare & Loer, 2004). Ub^{G76V}-GFP levels in null mutants for all three of these genes were similar to those in wild type in day 1 (L4 + 24 h) adults but remained stable in day 2 adults (Fig 2K; Appendix Fig S4), suggesting reduced turnover. BAS-1 synthesizes 5-HT and DA from 5-hydroxytryptophan (5-HTP) and L-DOPA (Fig 2A), respectively, so this result suggests that these neurotransmitter intermediates are not sufficient to substitute in UPS regulation for their canonical biogenic amine products. Although these mutants block signaling of multiple biogenic amines, their effect on Ub^{G76V}-GFP turnover was not greater than that of mutants defective in signaling from single biogenic amines, suggesting that DA, 5-HT, and TA might regulate UPS activity through a single, shared genetic and physiological process.

Finally, we characterized receptor mutants for the two best studied biogenic amines, 5-HT and DA, in *C. elegans*. Four DA receptors (*dop-1*, *dop-2*, *dop-3*, and *dop-4*) mediate DA signaling, whereas four 5-HT receptors (*ser-1*, *ser-5*, *ser-7*, and *mod-1*) mediate 5-HT signaling (Chase & Koelle, 2007). Mutants for *dop-1* and *dop-4* showed decreased turnover of Ub^{G76V}-GFP (Fig 2L), similar to previous observations (Joshi et al, 2016). Mutants for *ser-1*, *ser-5*, and *mod-1*, but not *ser-7*, also had stabilized Ub^{G76V}-GFP levels (Fig 2L and Appendix Fig S4). Serotonin regulates multiple physiological systems in *C. elegans*, including pharyngeal pumping rate, fat

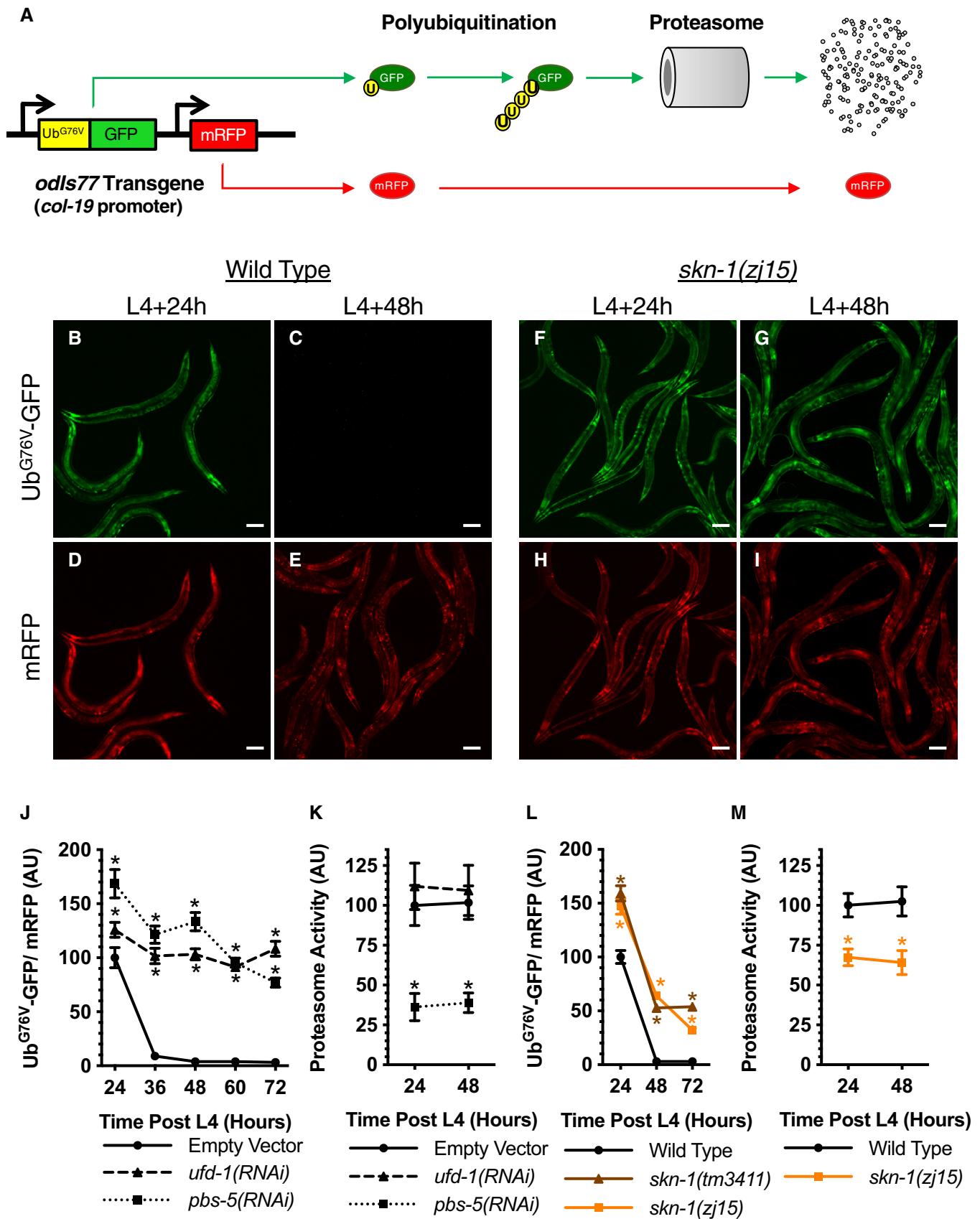


Figure 1.

Figure 1. The Ub^{G76V}-GFP transgene reports UPS activity.

- A Schematic representation of the Ub^{G76V}-GFP chimeric reporter (yellow for ubiquitin and green for GFP) and its associated mRFP internal control (red). The Ub^{G76V}-GFP chimera, which contains a mutation in the terminal residue of ubiquitin, cannot be cleaved. The resulting protein is a substrate for poly-ubiquitination (indicated by the circles labeled with "u") and degradation by the proteasome. High levels of reporter poly-ubiquitination and/or proteasome activity result in little or no GFP fluorescence.
- B, C Expression via the *col-19* promoter of Ub^{G76V}-GFP in *C. elegans* hypodermis from a single integrated transgene at (B) L4 + 24 h and (C) L4 + 48 h. Wild-type animals are shown. Scale bar, 100 μ m.
- D, E Expression of mRFP in the same animals as (B, C) at (D) L4 + 24 h and (E) L4 + 48 h. Scale bar, 100 μ m.
- F, G Expression via the *col-19* promoter of Ub^{G76V}-GFP in *C. elegans* hypodermis from a single integrated transgene at (F) L4 + 24 h and (G) L4 + 48 h. Mutants for *skn-1(zj15)* are shown. Scale bar, 100 μ m.
- H, I Expression of mRFP in the same animals as (F, G) at (H) L4 + 24 h and (I) L4 + 48 h. Scale bar, 100 μ m.
- J Quantified fluorescence of Ub^{G76V}-GFP normalized to mRFP in the hypodermis of animals from the indicated time point (in hours) after the L4 stage. Animals were exposed to the indicated knockdown RNAi bacterial strains or a strain that only contained the empty RNAi vector since hatching. **P* < 0.001 using ANOVA with Dunnett's *post hoc* comparison to the wild-type control equivalent time point, with *N* = 20 animals per genotype and time point. Error bars indicate SEM.
- K Quantified epoxomicin-sensitive proteasome activity (difference in slope of turnover of fluorescent chymotrypsin substrate between epoxomicin-treated and untreated samples; see Appendix Fig S2) from lysates of animals treated as in (J). **P* < 0.001, using ANOVA with Dunnett's *post hoc* comparison to the empty RNAi vector control, with *N* = 3 trials. Error bars indicate SEM.
- L Quantified fluorescence of Ub^{G76V}-GFP normalized to mRFP in the hypodermis of animals from the indicated time point (in hours) and the indicated genotypes after the L4 stage, as per (J). **P* < 0.001 using ANOVA with Dunnett's *post hoc* comparison to the wild-type control equivalent time point, with *N* = 20 animals per genotype and time point. Error bars indicate SEM.
- M Quantified epoxomicin-sensitive proteasome activity, as per (K). **P* < 0.001 using ANOVA with Dunnett's *post hoc* comparison to the wild-type control equivalent time point, with *N* = 3 trials. Error bars indicate SEM.

accumulation, and egg laying, through the use of distinct receptor combinations (Chase & Koelle, 2007). We did not observe defects in pumping or egg laying in *cat-2* and *tdc-1* mutants (Appendix Fig S5), suggesting that defects in these systems are not the cause of the UPS phenotype in these mutants. By contrast, mutants for the 5-HT receptor *ser-7* are defective in pumping, egg laying, and fat accumulation, yet do not have a UPS phenotype (Carre-Pierrat et al, 2006; Hobson et al, 2006; Yemini et al, 2013). Thus, a novel combination of 5-HT receptors, distinct from those that regulate these other physiological systems, mediates UPS regulation.

Biogenic amine signaling promotes protein poly-ubiquitination without perturbing proteasome chymotrypsin-like activity

The stabilization of Ub^{G76V}-GFP protein in biogenic amine signaling mutants could be due to either a reduction in its poly-ubiquitination or a reduction in its proteolysis by the proteasome. We made lysates from different biogenic amine synthesis mutants at day 2 of adulthood (L4 + 48 h), separated proteins on two different SDS-PAGE gels, and then detected Ub^{G76V}-GFP protein by Western blot either with anti-GFP antibodies (Fig 3A) or anti-ubiquitin antibodies (Fig 3B). Little Ub^{G76V}-GFP protein is detected in wild-type animals or *tbh-1* mutants at L4 + 48 h (quantified in Fig 3C and D). Our control *skn-1(zj15)* mutants accumulated non-ubiquitinated, mono-ubiquitinated, di-ubiquitinated, and tri-ubiquitinated Ub^{G76V}-GFP species, reflecting a reduction in poly-ubiquitination and/or the ability to clear poly-ubiquitinated substrates, consistent with reduced proteasome activity in these mutants (Fig 3A–D). We observed a similar pattern of ubiquitinated Ub^{G76V}-GFP accumulation in *cat-2*, *tdc-1*, and *tph-1* mutants. While we did not detect proteins larger than 70 kDa in biogenic signaling mutants or *skn-1(zj15)* using the anti-GFP antibodies (Fig 3A), we did detect additional proteins ranging from 70 to 250 kDa in these mutants using anti-ubiquitin antibodies (Figs 3B and E, and EV2), which detects endogenous ubiquitinated proteins in addition to the Ub^{G76V}-GFP reporter. Although we cannot determine whether such proteins are mono-, di-, or poly-ubiquitinated, our results suggest that ubiquitinated

forms of endogenous proteins accumulate in these mutants. As additional confirmation, we also examined animals lacking the *odIs77* transgene and observed a similar accumulation of endogenous ubiquitinated protein (Fig EV2). Together, these results suggest that DA, 5-HT, and TA signaling promote either protein ubiquitination, proteolysis by the proteasome, or both.

We also directly examined chymotrypsin-like proteasome activity in biogenic signaling mutants. We generated lysates of L4 + 48 h nematodes and first analyzed Ub^{G76V}-GFP and mRFP levels in these lysates by fluorescence spectroscopy (Fig 3F). We observed low levels of Ub^{G76V}-GFP fluorescence at L4 + 48 h in wild-type and *tbh-1* mutant animals, similar to what we observed by epifluorescence microscopy and Western blot analysis. By contrast, Ub^{G76V}-GFP fluorescence was elevated in *cat-2*, *tph-1*, *tdc-1*, and *skn-1* mutants (Fig 3F). We incubated the same lysates with the fluorescent chymotryptic substrate Suc-Leu-Leu-Val-Tyr-AMC to measure epoxomicin-sensitive proteasome activity. As expected, *skn-1(zj15)* control lysates showed reduced activity (Fig 3G), which is in consonance with our quantification by epifluorescence microscopy (Fig 1). We did not observe a substantial change in proteasome chymotrypsin-like activity in any of the biogenic amine mutants compared with wild type. We cannot rule out the possibility that some other aspect of the 26S proteasome (e.g., other 20S protease activities, substrate recognition and unfolding by the 19S subunit, the activity of proteasome-associated deubiquitinating enzymes, or the activity of substrate shuttling factors) is modified in these mutants such that its capacity to remove Ub^{G76V}-GFP is reduced (Collins & Goldberg, 2017). Nevertheless, when taken together, the accumulation of Ub^{G76V}-GFP species with reduced ubiquitin valence (i.e., the shift from poly-ubiquitinated to non-ubiquitinated, mono-ubiquitinated, and di-ubiquitinated forms), combined with no observed change in proteasome activity in *cat-2*, *tph-1*, and *tdc-1* mutants, strongly suggests that DA, 5-HT, and TA signaling does not regulate chymotrypsin-like proteasome activity but instead either promotes the poly-ubiquitination of unstable proteins like Ub^{G76V}-GFP or facilitates the ability of the proteasome to access such proteins.

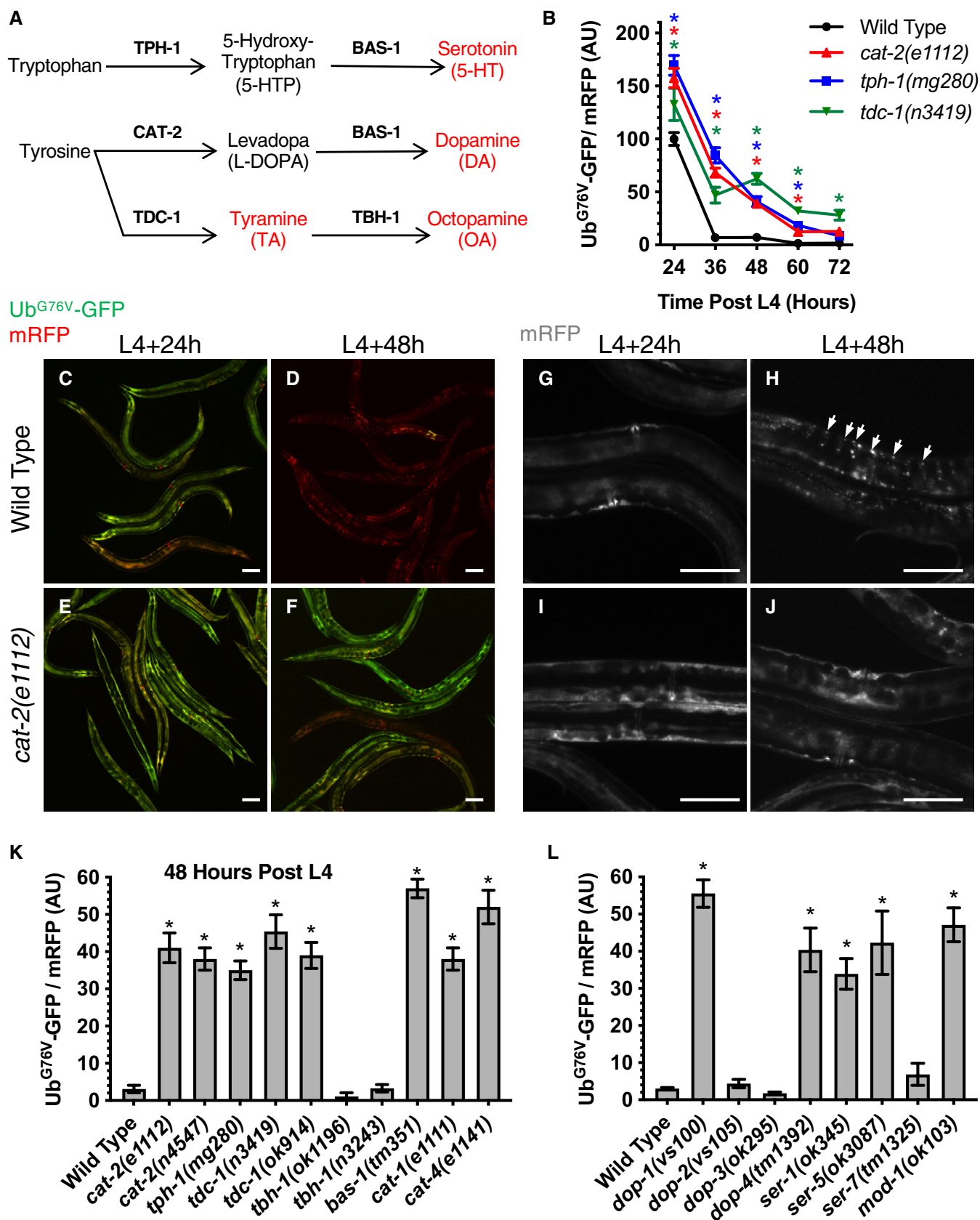


Figure 2.

Figure 2. Biogenic amine signaling modulates protein turnover.

- A Schematic representation of the biogenic amine synthesis pathways in *Caenorhabditis elegans*. Final biogenic amine neurotransmitter products are shown in red. The gene encoding each biosynthesis enzyme in the pathway is indicated over the arrow representing its catalyzed reaction.
- B Quantified fluorescence of Ub^{G76V}-GFP normalized to mRFP in the hypodermis of animals of the specified genotype from the indicated time point (in hours) after the L4 stage. **P* < 0.001 using ANOVA with Dunnett's *post hoc* comparison to the wild-type control equivalent time point, with *N* = 20 animals per genotype and time point. Error bars indicate SEM.
- C, D Co-expression via the *col-19* promoter of Ub^{G76V}-GFP (green) and mRFP (red) in *C. elegans* hypodermis from a single integrated transgene at (C) L4 + 24 h and (D) L4 + 48 h. Green and red channels are merged. Wild-type animals are shown. Scale bar, 100 μm.
- E, F Similar analysis as in (C, D) for *cat-2(e1112)* mutants. Scale bar, 100 μm.
- G, H Expression of mRFP via the *col-19* promoter in *C. elegans* hypodermis at (G) L4 + 24 h or (H) L4 + 48 h. Wild-type animals are shown. Puncta containing mRFP aggregates are indicated by arrows. Scale bar, 100 μm.
- I, J Similar analysis as in (G, H) for *cat-2(e1112)* mutants. Scale bar, 100 μm.
- K, L Quantified fluorescence of Ub^{G76V}-GFP normalized to mRFP in the hypodermis of animals of the indicated genotype at L4 + 48 h. **P* < 0.001 using ANOVA with Dunnett's *post hoc* comparison to the wild-type control equivalent time point, with *N* = 20 animals per genotype and time point. Data have been normalized to wild type. Error bars indicate SEM.

Biogenic amine signaling promotes expression of cytochrome P450 enzymes and eicosanoids

Biogenic amine signaling results in both transcriptional and post-translational changes to other signaling pathway components (Roeder, 2005; Mohammad-Zadeh *et al*, 2008; Frederick & Stanwood, 2009; Klein *et al*, 2019). We reasoned that the long-term changes in UPS activity and proteostasis in biogenic amine mutants could reflect differences in gene expression. We compared the mRNA expression profile of the four biogenic amine mutants to wild-type animals in day 2 (L4 + 48 h) adults using RNA-seq. We isolated poly-A(+) RNA from three replicates of each genotype, subjected each sample to whole transcriptome sequencing (RNA-seq), aligned resulting reads to the *C. elegans* genome using STAR (Dobin *et al*, 2013), and assessed differential gene expression between genotypes using EdgeR and an FDR-adjusted *q*-value (Anders & Huber, 2010), focusing only on genes with significant changes (*q* < 0.01, 2-fold or more, lower or higher, compared to wild type) (Dataset EV1). Expression levels for Ub^{G76V}-GFP and mRFP mRNAs were similar to those for *col-19*, consistent with the use of the *col-19* promoter for these transgenes, and they were similar in the different biogenic amine mutants (Appendix Fig S6). Mutants for *cat-2* and *tdc-1* had the greatest number of differentially expressed genes, whereas *tph-1* and *tbh-1* mutants had more modest numbers of differentially expressed genes (Appendix Fig S6). Less than 1% of differentially expressed genes were commonly regulated in all four genotypes, but about 20% were commonly regulated in at least three genotypes (Appendix Fig S6). We used DAVID functional annotation clustering enrichment analysis (Huang da *et al*, 2009a; Huang da *et al*, 2009b) to examine gene ontology and pathway enrichment for genes enriched in one or more of the genotypes (Fig 4A). Although there was little gene ontology or pathway enrichment in genes that were overexpressed in any of the mutants relative to wild type, we observed high DAVID enrichment scores for multiple ontology groups in genes that were underexpressed in one or more mutants. For example, genes involved in cuticle structure were enriched in the pool of downregulated genes observed in *tdc-1* mutants, suggesting a role for TA in cuticle formation and function. Multiple chloride channels were enriched in the downregulated genes found in both *cat-2* and *tdc-1* mutants, suggesting a role for DA and TA in promoting chloride channel synthesis.

As Ub^{G76V}-GFP turnover was reduced in *cat-2*, *tph-1*, and *tdc-1* mutants, we were particularly interested in genes enriched in differentially expressed profiles from all three of these mutants. We noticed a large set of commonly regulated genes between these three genotypes (21% of *cat-2* genes, 35% of *tph-1* genes, and 28% of *tdc-1* genes; Appendix Fig S6). This gene set was enriched for chitin metabolism, glycosyltransferases, and cytochrome P450 monooxygenases (Fig 4A), suggesting that one or more of these biological processes might be involved in a mechanism of UPS-mediated proteostasis shared by the three mutants.

We focused on cytochrome P450 proteins, which comprise a diverse superfamily of heme-containing enzymes involved in xenobiotic detoxification, fatty acid and steroid oxidation, and hormone synthesis and breakdown (Denisov *et al*, 2005; McLean *et al*, 2005). The *C. elegans* genome contains 75 cytochrome P450 (CYP) genes assigned to 16 independent families within the CYP superfamily (Gotoh, 1998; Kulas *et al*, 2008). Most of the nematode CYP genes are similar to members of the mammalian CYP1/2, CYP3, and CYP4 families. We examined the expression of all *C. elegans* CYP genes in the biogenic amine mutants and found that the levels of the CYP14, CYP29, and CYP34 subfamily members were commonly underexpressed, as indicated by low log fold change, in *cat-2*, *tph-1*, and *tdc-1* mutants (Fig 4B). These enzymes are closely related to the CYP2 and CYP4 microsomal monooxygenases, which produce eicosanoid signaling molecules and second messengers from long-chain PUFAs (McGiff & Quilley, 1999; Capdevila *et al*, 2000; Zeldin, 2001; Roman, 2002; Kulas *et al*, 2008; Spector & Kim, 2015).

If DA, 5-HT, and TA synthesis are required to promote the expression of CYP14, CYP29, and CYP34 genes, then do these biogenic amines promote the production of eicosanoids from PUFAs? *C. elegans* contains a complete set of genes to produce *n*-6 (ω6) and *n*-3 (ω3) long-chain PUFAs (Fig 4C), including arachidonic acid (AA) and eicosapentaenoic acid (EPA), from oleic acid (OA) (Wallis *et al*, 2002; Watts & Browse, 2002; Vrablik & Watts, 2013; Ying & Zhu, 2016). We tested this hypothesis by collecting and lysing synchronized day 2 adult nematodes, followed by either direct LC-MS analysis (for free fatty acid extraction) or alkaline hydrolysis and LC-MS analysis (for total fatty acid extraction). Free AA-derived *n*-6 eicosanoids (Fig 4D) were about 100-fold less abundant compared with free EPA-derived *n*-3 eicosanoids (Fig 4E), as previously observed (Kulas *et al*, 2008). As controls, we measured eicosanoid levels in *fat-1* mutants, which fail to

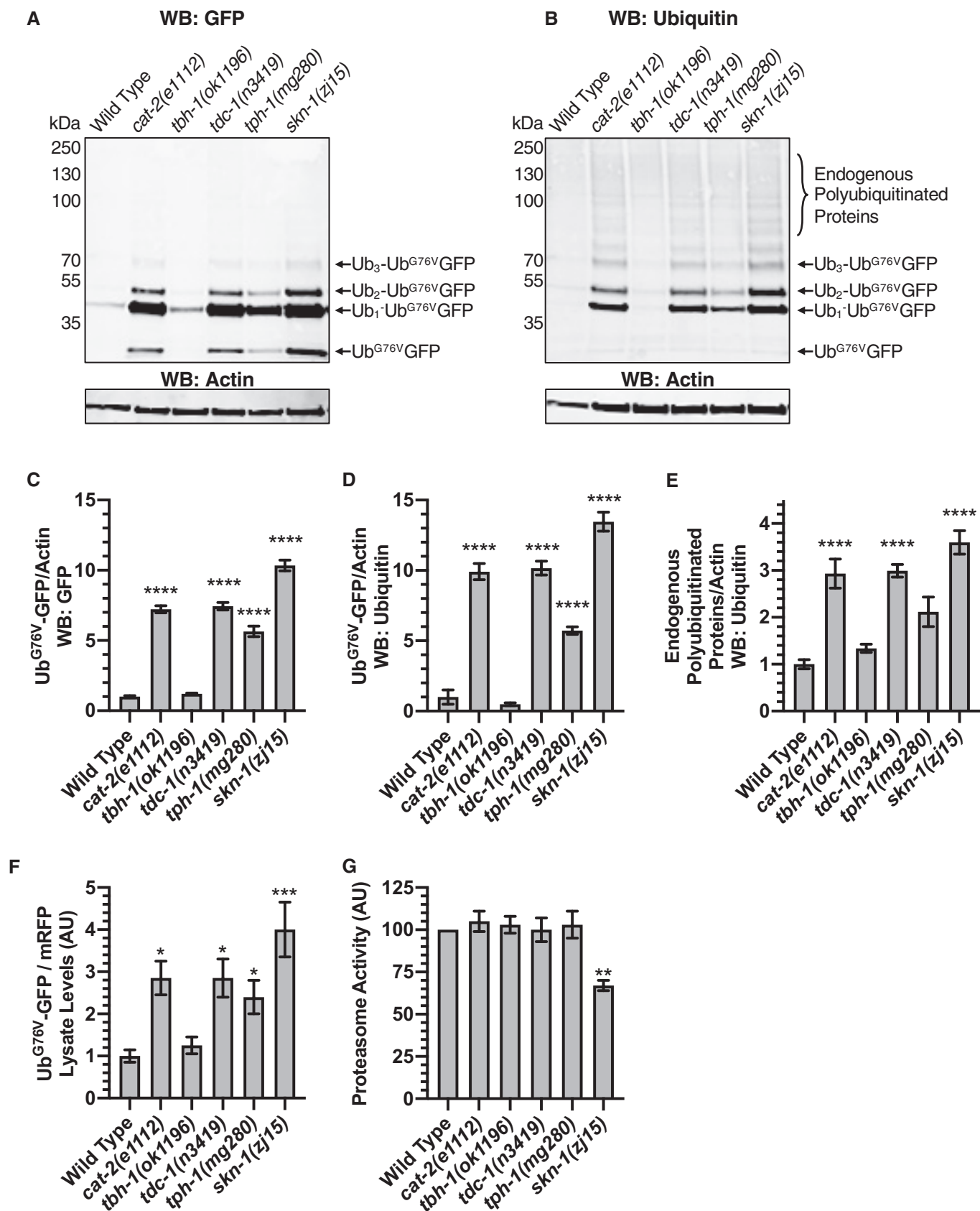


Figure 3.

Figure 3. Biogenic amine signaling promotes protein poly-ubiquitination without perturbing proteasome function.

- A Western blot of lysed transgenic nematodes that express the Ub^{G76V}-GFP and mRFP reporters in the hypodermis at the L4 + 48 h stage, probed with antibodies recognizing GFP or actin as a loading control. The position of molecular weight markers is shown on the left of each blot. The position of Ub^{G76V}-GFP protein, as well as Ub^{G76V}-GFP with the indicated number of additional ubiquitin moieties, based on molecular weight, is indicated to the right of each blot. Twenty animals were loaded per lane for each indicated genotype.
- B A separate SDS-PAGE and Western blot of the same lysates from (A), probed with antibodies recognizing ubiquitin or actin as a loading control. The position of molecular weight markers is shown on the left of each blot. The position of Ub^{G76V}-GFP protein, as well as Ub^{G76V}-GFP with the indicated number of additional ubiquitin moieties, based on molecular weight, is indicated to the right of each blot. Endogenous poly-ubiquitinated proteins are also detected in the 80–200 kDa range, as indicated by the bracket. Twenty animals were loaded per lane for each indicated genotype.
- C Quantified Ub^{G76V}-GFP protein levels relative to actin control for each indicated lane for the blot in (A). *****P* < 0.0001, ANOVA with Dunnett's *post hoc* comparison to wild type. *N* = 3 trials. Error bars indicate SEM.
- D Quantified Ub^{G76V}-GFP protein levels relative to actin control for each indicated lane for the blot in (B). *****P* < 0.0001, ANOVA with Dunnett's *post hoc* comparison to wild type. *N* = 3 trials. Error bars indicate SEM.
- E Quantified endogenous poly-ubiquitinated protein levels relative to actin control for each indicated lane for the blot in (B). *****P* < 0.0001, ANOVA with Dunnett's *post hoc* comparison to wild type. *N* = 3 trials. Error bars indicate SEM.
- F Quantified fluorescence of Ub^{G76V}-GFP normalized to mRFP from the same lysates. **P* < 0.01, ****P* < 0.001, ANOVA with Dunnett's *post hoc* comparison to wild type. *N* = 3 trials. Error bars indicate SEM.
- G Quantified epoxomicin-sensitive proteasome activity (as measured through the turnover of fluorescent chymotrypsin substrate) from the same lysates. ***P* < 0.01, ANOVA with Dunnett's *post hoc* comparison to the wild-type control, with *N* = 3 trials. Error bars indicate SEM.

synthesize *n*-3 long-chain PUFAs, and *fat-4* mutants, which fail to synthesize AA and EPA from dihomo- γ -linolenic acid (DGLA) and eicosatetraenoic acid (ETA) PUFAs, respectively (Watts & Browse, 2006). Mutants for *fat-4* lacked both AA- and EPA-derived eicosanoids (Fig 4D and E). Mutants for *fat-1* lacked EPA-derived eicosanoids but accumulated an unusually high level of AA-derived eicosanoids, perhaps due to the redirection of PUFAs into AA-derived eicosanoids. We focused on the two best studied biogenic amines, DA and 5-HT, measuring eicosanoid levels in *cat-2* and *tph-1* mutants, respectively. We found a significant reduction in both AA- and EPA-derived free eicosanoids in both mutants (Fig 4D and E), indicating that DA and 5-HT biogenic amines promote the synthesis of these lipid signaling molecules. Our analysis of individual eicosanoids from both the total and the free fatty acid extraction methods yielded similar results (Appendix Figs S7 and S8).

The cytochrome P450 CYP-34A4 promotes UPS activity

If biogenic amine signaling regulates the UPS by promoting CYP microsomal monooxygenase expression and eicosanoid synthesis, then mutations in one or more of these CYP genes should impair this UPS regulation. Several mutations predicted to change conserved residues for one of these genes, *cyp-34A4* (Fig 5A), were available from the Million Mutation collection (Thompson *et al*, 2013), providing potential tools to analyze *cyp-34A4* function. The mRNA levels for *cyp-34A4* were significantly reduced in *cat-2*, *tph-1*, and *tdc-1* mutants, but not in *tbh-1* mutants (Fig 5B). We mapped the amino acid changes for these mutations on an alignment between CYP-34A4 and the closely related rabbit CYP2C5 and human CYP2C8 (Appendix Fig S9), for which there is extensive biochemical and structural data (Williams *et al*, 2000; Schoch *et al*, 2004). The *gk933903* mutation changes a conserved proline to serine (P26S) in a loop that forms the membrane-binding surface (Fig 5A; Appendix Fig S9). The *gk690081* mutation changes a conserved glycine to arginine (G395R) in the beta sheet structure that forms the membrane-binding surface and helps coordinate lipid substrate interaction. The *gk759290* mutation changes a key conserved glycine to

glutamate (G482E) at the end of a loop that helps stabilize helices that interact with lipid substrates. We introduced the *odIs77* transgene into these mutants and observed Ub^{G76V}-GFP stabilization (Fig 5C; Appendix Fig S10), similar to *cat-2*, *tph-1*, and *tdc-1* mutants, demonstrating that at least one of the CYP genes whose expression is elevated by biogenic amine signaling is required to modulate UPS activity.

As an independent confirmation, we used CRISPR/Cas9-mediated genome editing to introduce a small genomic rearrangement into *cyp-34A4*. This allele, *od107*, deletes 129 bases of the first two exons and the first intron, inserting 51 bases of novel DNA in its place. The rearrangement results in the deletion of amino acids 18–46, which encodes the N-terminal coil that forms the predicted membrane-binding surface (Fig 5A; Appendix Fig S9). Following amino acid 17, *od107* creates two novel proline residues followed by a nonsense codon terminating translation of *cyp-34A4*, making this allele a likely null. We introduced *odIs77* into this mutant and observed stabilized Ub^{G76V}-GFP in day 2 (L4 + 48 h) adults (Fig 5C), similar to the other alleles of this gene. We did not observe differences compared with wild type in pharyngeal pumping, egg laying, or developmental timing for any *cyp-34A4* mutants, suggesting that the change in Ub^{G76V}-GFP turnover is unlikely to be due indirectly to defects in one of these processes (Appendix Fig S11). We had observed that supplementation of growth media of *cat-2* and *tph-1* with DA and 5-HT rescued those mutants for their UPS phenotype and that supplementing 5-HT in the growth media of wild-type animals resulted in precocious Ub^{G76V}-GFP turnover (Fig EV1). By contrast, supplementation with DA or 5-HT failed to rescue *cyp-34A4* mutants, and *cyp-34A4* mutations blocked the precocious Ub^{G76V}-GFP turnover triggered by 5-HT supplementation (Fig EV3). Taken together, our results demonstrate that DA, 5-HT, and TA normally promote CYP-34A4 expression and that CYP-34A4 is required for UPS activation in day 2 adults.

Many cytochrome P450 enzymes interact with cytochrome P450 reductase, which allows electron transfer from NAD(P)H to reduce ferric P450 heme, to split oxygen, and then to hydroxylate substrate (McLean *et al*, 2005). EMB-8 encodes the lone *C. elegans* NADPH-cytochrome P450 reductase, and the mutation *emb-8*

(*hc69*) is a loss-of-function mutation that gives a conditional embryonic lethal phenotype (Miwa *et al*, 1980; Rappleye *et al*, 2003). We introduced the *odIs77* UPS reporter transgene into *emb-8* mutants and then hatched wild-type and *emb-8* mutants

harboring the transgene at a permissive temperature (15°C). When synchronized animals reached the L4 stage, we shifted to a restrictive temperature (20°C) and observed Ub^{G76V}-GFP fluorescence. We found that Ub^{G76V}-GFP was stable in *emb-8* day 2 (L4 + 48 h)

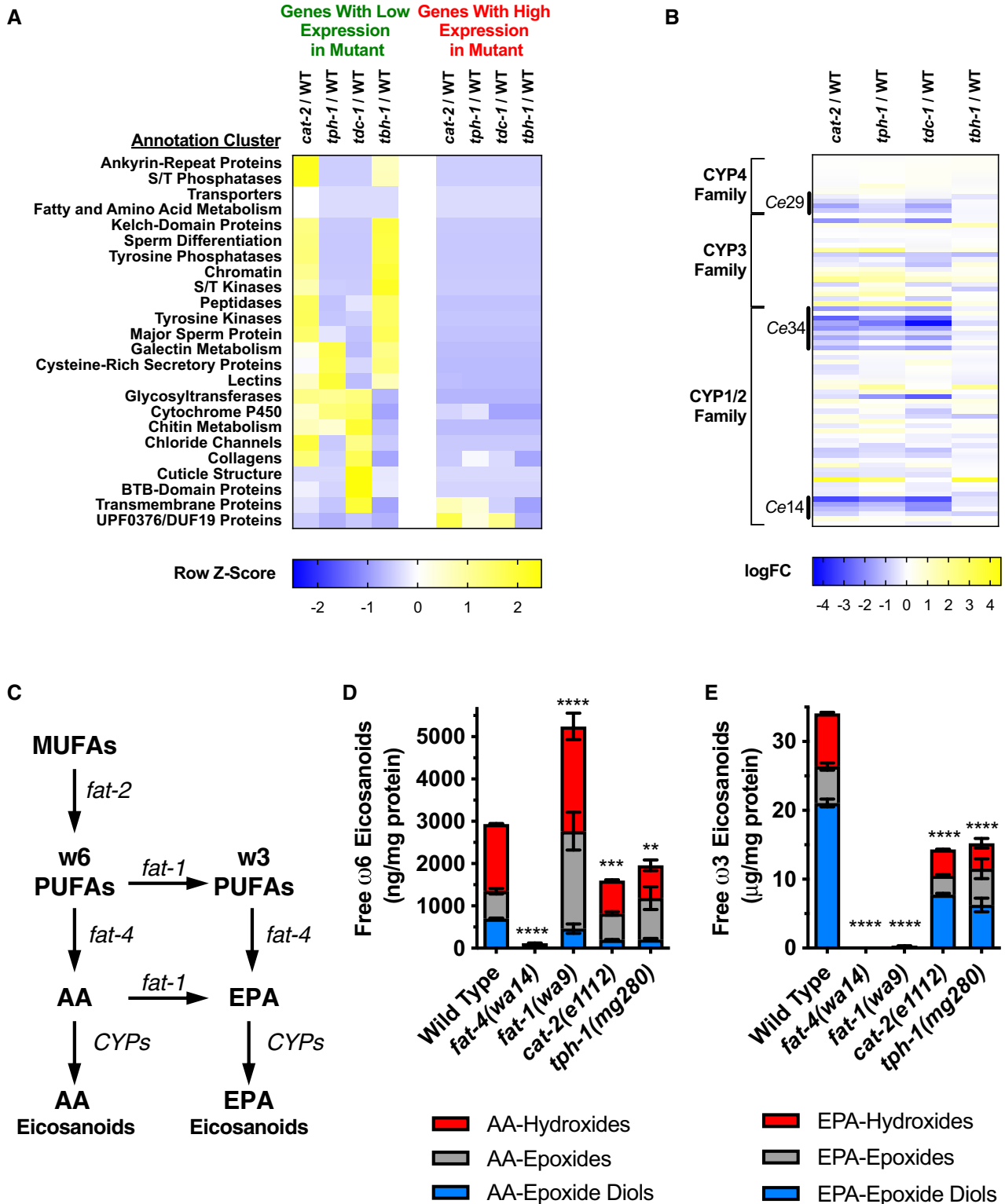


Figure 4. Biogenic amine signaling promotes expression of cytochrome P450 enzymes and eicosanoids.

- A Heat map of DAVID analysis showing enriched annotation clusters (e.g., gene ontology and pathways) in the genes showing differential expression between the indicated mutant and wild type. Each annotation cluster is represented by a DAVID annotation cluster score (the higher the number, the stronger the enrichment). DAVID analysis of genes whose expression is lower in a mutant relative to wild type is highlighted with green text (four left-hand columns), whereas DAVID analysis of genes whose expression is higher in a mutant relative to wild type is highlighted with red text (four right-hand columns). Rows are labeled with each annotation cluster, with Z-scores (color scale at graph bottom) representing significant deviation in the annotation cluster score between genotypes across the row for each annotation cluster. Yellow cells indicate higher-than-average enrichment of that annotation cluster (row) for that genotypic comparison (column). Annotation clusters (rows) are further clustered along the Y-axis according to the Pearson average linkage method.
- B Heat map of log fold change (logFC, color scale at graph bottom) in the expression of *C. elegans* CYP genes between the indicated mutant and wild type. Genes whose expression is lower in a mutant relative to wild type are colored blue, whereas genes whose expression is higher in a mutant relative to wild type are colored yellow. Rows are labeled for the different CYP families and subfamilies. Specific genes (rows) are clustered according to sequence alignment (CLUSTAL W) to maintain the relationship of their molecular evolution.
- C Schematic representation of the synthesis pathway for mono-unsaturated fatty acids (MUFAs), poly-unsaturated fatty acids (PUFAs), arachidonic acid (AA), eicosapentaenoic acid (EPA), and their derived eicosanoids in *C. elegans*. The gene encoding each biosynthesis enzyme in the pathway is indicated next to the arrow representing its catalyzed reaction.
- D Abundance of the indicated free $\omega 6$ PUFA-derived eicosanoid, normalized to total protein, for each indicated genotype. Red, gray, and blue stacked bars indicate hydroxides, epoxide, and epoxide diol forms of eicosanoids, respectively. **** $P < 0.0001$, *** $P < 0.001$, ** $P < 0.01$, ANOVA with Dunnett's *post hoc* comparison to wild type. $N = 3$ trials. Error bars indicate SEM.
- E Abundance of the indicated free $\omega 3$ PUFA-derived eicosanoid, as in (D), normalized to total protein, for each indicated genotype. Red, gray, and blue stacked bars indicate hydroxides, epoxide, and epoxide diol forms of eicosanoids, respectively. **** $P < 0.0001$, ANOVA with Dunnett's *post hoc* comparison to wild type. $N = 3$ trials. Error bars indicate SEM.

adults (Fig 5D; Appendix Fig S10), similar to *cyp-34A4* mutants. These results demonstrate that the cytochrome P450 reductase activity is required for UPS regulation and that CYP-34A4 likely works with this reductase to oxidize one or more key substrates involved in that regulation.

To examine CYP-34A4 expression more closely, we generated a translational reporter containing the complete transcription unit and 2 kb of upstream sequence fused in frame to Venus at the CYP-34A4 C-terminus. We introduced this resulting transgene into the *C. elegans* germline and observed expression only in the intestine (Fig 5E and F), with consistent expression through larval stages into adulthood, suggesting that CYP-34A4 might act non-autonomously to influence UPS proteostasis in hypodermal tissues. Although we do not observe CYP-34A4 expression in tissues other than the intestine, a cell autonomy experiment would be required to demonstrate this point formally.

PUFAs modulate UPS activity

If the enzymatic role of CYP-34A4 in UPS regulation is eicosanoid production rather than small-molecule xenobiotic detoxification, then mutations that disrupt PUFA synthesis should cause the same Ub^{G76V}-GFP stabilization phenotype observed in *cyp-34A4* and biogenic amine mutants. In *C. elegans*, PUFAs are generated from the mono-unsaturated fatty acid (MUFA) oleic acid (OA) by the $\Delta 12$ -fatty acid desaturase FAT-2 (Fig 6A), and *fat-2* mutants lack normal PUFAs (Peyou-Ndi et al, 2000; Watts & Browse, 2002). We introduced *odIs77* into *fat-2(ok873)* mutants, which have a deletion within *fat-2*, and observed stabilization of Ub^{G76V}-GFP, similar to *cyp-34A4* mutants (Fig 6B), suggesting that long-chain PUFAs and their eicosanoid derivatives are required for Ub^{G76V}-GFP turnover.

Serotonin promotes the mobilization and beta oxidation of stored fats (lipid droplet triglycerides) in the intestine, with *tph-1* mutants accumulating triglycerides but not phospholipids. Although *cat-2* mutants do not accumulate stored fat, it remained possible that augmented triglyceride storage rather than depressed eicosanoid production explained the UPS phenotype in *tph-1* mutants (Srinivasan et al, 2008; Alberti et al, 2010; Noble et al, 2013; Barros et al,

2014). Eicosanoids are derived from phospholipids rather than triglyceride stores; nevertheless, we examined mutants with variable levels of stored fats to determine whether fat storage correlated with UPS activity. The transcription factor NHR-49 promotes the expression of enzymes involved in beta oxidation of triglyceride stores as well as enzymes that mediate desaturation and elongation required to synthesize long-chain PUFAs and their eicosanoid derivatives (Ashrafi et al, 2003; Van Gilst et al, 2005; Taubert et al, 2006). The $\Delta 9$ -fatty acid desaturase FAT-7 not only promotes the formation of MUFAs and PUFAs (and their eicosanoid derivatives) from saturated fatty acids, but it also inhibits triglyceride beta oxidation. Eicosanoids are reduced in both *nhr-49* and *fat-7* mutants; however, *nhr-49* mutants accumulate fat stores, whereas *fat-7* mutants are depleted for such stores. We found that both *nhr-49* and *fat-7* mutants had reduced Ub^{G76V}-GFP turnover and UPS activity (Fig 6C), consistent with their reduced level of eicosanoids but inconsistent with a model in which the mobilization of fat stores regulates UPS activity.

In order to examine nematodes in which eicosanoids are selectively removed, we introduced *odIs77* into *fat-4(wa14)* mutants, which contain a nonsense mutation in the FAT-4 $\Delta 5$ -fatty acid desaturase and lack AA, EPA, and all eicosanoids derived from these PUFAs (Figs 4D and E, and 6A) (Watts & Browse, 2002). We did not observe Ub^{G76V}-GFP stabilization at L4 + 48 h, instead observing precocious turnover of the UPS reporter at L4 + 24 h (Fig 6B). We also introduced *odIs77* into *fat-1(wa9)* mutants, which contain a nonsense mutation in the FAT-1 *n-3*-fatty acid desaturase, lack EPA and *n-3* eicosanoids from EPA, and accumulate AA and *n-6* eicosanoids (Figs 4D and E, and 6A; Watts & Browse, 2002). We observed an even more dramatic precocious turnover of Ub^{G76V}-GFP in these mutants (Fig 6B). Double mutants between *fat-1* and *fat-4* resembled *fat-4* mutants (Fig 6B), indicating that *fat-4* is epistatic to *fat-1* and that the accumulation of AA or one of its eicosanoid derivatives might be responsible for the strong precocious turnover of Ub^{G76V}-GFP in *fat-1* single mutants. Interestingly, *fat-3(ok1126)* mutants showed a similar precocious turnover phenotype to that of *fat-4* mutants (Fig 6B). These mutants contain a deletion for the FAT-3 $\Delta 3$ -fatty acid desaturase, accumulate linoleic acid (LA), and alpha-

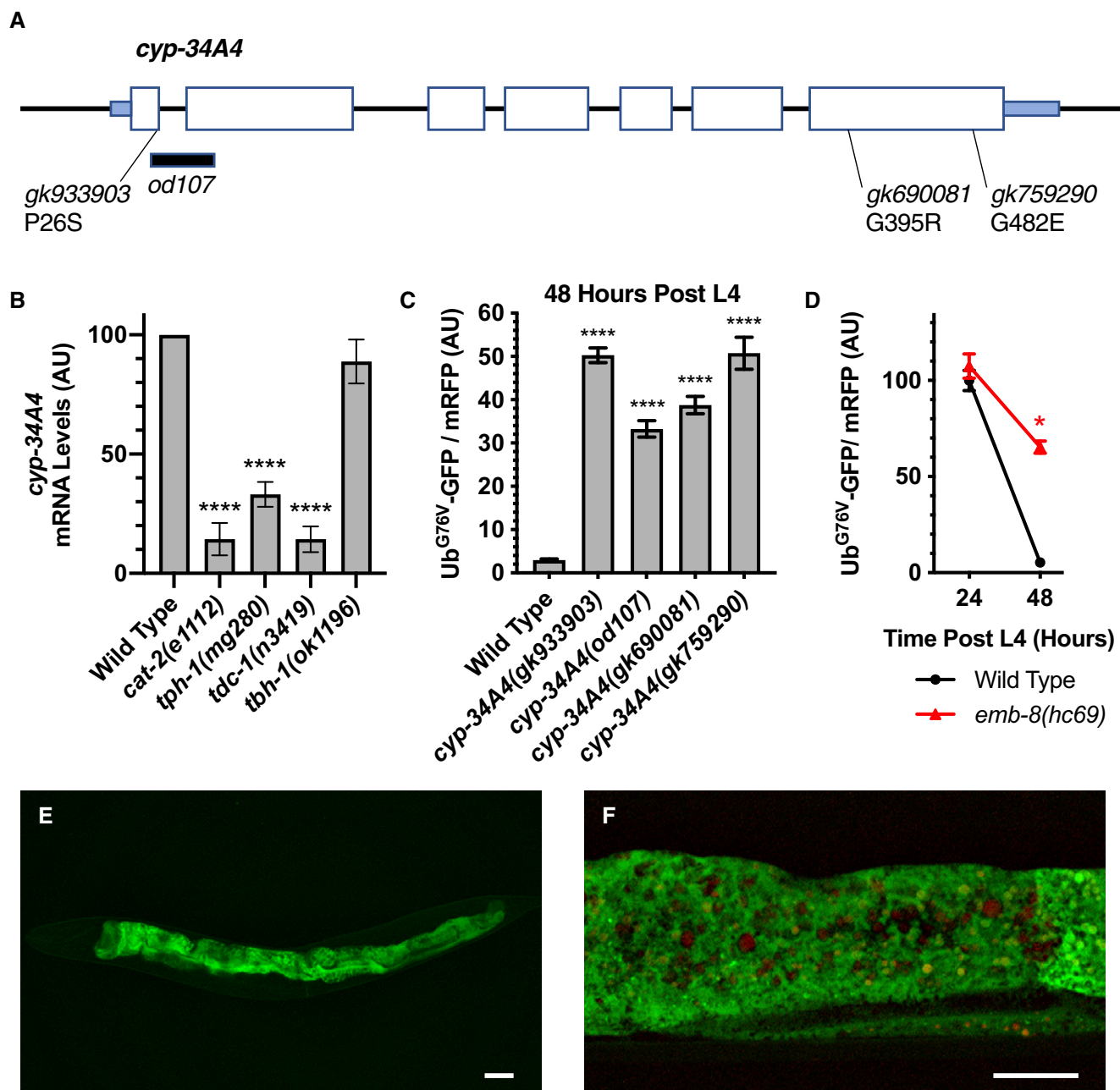


Figure 5. The cytochrome P450 CYP-34A4 promotes UPS activity.

- A Schematic of the *cyp-34A4* gene. Large boxes indicate coding sequences. Small boxes indicate UTRs. The location and nature of individual mutations is shown. Sequence deleted in *od107* is shown with a horizontal black bar.
- B Relative abundance of mRNA for the *cyp-34A4* gene. Values are based on qRT-PCR analysis, with the relative levels for each gene normalized to the value observed in the wild-type control. *** $P < 0.001$, ANOVA with Dunnett's *post hoc* comparison to wild type. $N = 3$ trials. Error bars indicate SEM.
- C Quantified fluorescence of Ub^{G76V}-GFP normalized to mRFP in the hypodermis of animals of the indicated genotype at L4 + 48 h. **** $P < 0.001$, ANOVA with Dunnett's *post hoc* comparison to the wild-type control equivalent time point. $N = 20$ animals per genotype and time point. Error bars indicate SEM.
- D Quantified fluorescence of Ub^{G76V}-GFP normalized to mRFP, as in (C). **** $P < 0.001$, ANOVA with Dunnett's *post hoc* comparison to the wild-type control equivalent time point. $N = 20$ animals per genotype and time point. Error bars indicate SEM.
- E Expression of the *cyp-34A4::gfp* transgene. Scale bar, 100 μm .
- F Expression of the *cyp-34A4::gfp* transgene (green). Intestinal autofluorescence (red) can be distinguished. Scale bar, 100 μm .

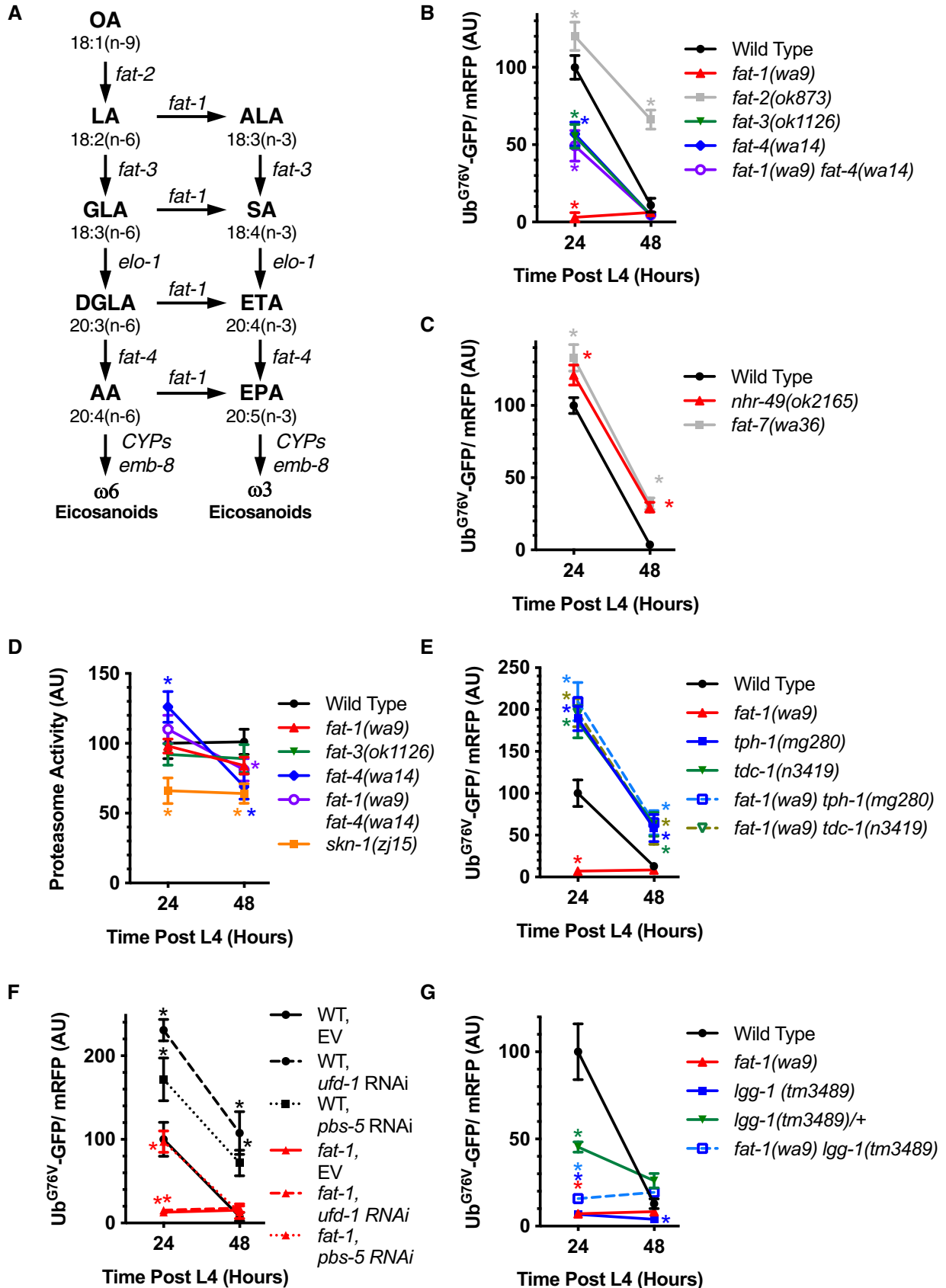


Figure 6.

Figure 6. PUFAs modulate UPS activity.

- A Schematic representation of the PUFA and eicosanoid synthesis pathways in *C. elegans*. Carbon chain length, double bond number, and double bond location along the chain are indicated for each PUFA. The gene encoding each biosynthesis enzyme in the pathway is indicated next to the arrow representing its catalyzed reaction.
- B, C Quantified fluorescence of Ub^{G76V}-GFP normalized to mRFP in the hypodermis of animals of the indicated genotype at the indicated time point. **P* < 0.001, ANOVA with Dunnett's *post hoc* comparison to the wild-type control equivalent time point. *N* = 20 animals per genotype and time point. Error bars indicate SEM.
- D Quantified epoxomicin-sensitive proteasome activity (as measured through the turnover of fluorescent chymotrypsin substrate) from lysates of the indicated genotype and time point. **P* < 0.001, ANOVA with Dunnett's *post hoc* comparison to the wild-type control equivalent time point. *N* = 3 trials. Error bars indicate SEM.
- E Quantified fluorescence as in (B) for animals of the indicated genotype at the indicated time point. **P* < 0.001, ANOVA with Dunnett's *post hoc* comparison to the wild-type control equivalent time point. *N* = 20 animals per genotype and time point. Error bars indicate SEM.
- F Quantified fluorescence as in (B) for animals exposed to the indicated RNAi vector or empty vector (EV) control, and in either a wild type (WT) or *fat-1(wa9)* genetic background. **P* < 0.001, ANOVA with Dunnett's *post hoc* comparison to the wild-type control equivalent time point. *N* = 20 animals per genotype and time point. Error bars indicate SEM.
- G Quantified fluorescence as in (B) for animals of the indicated genotype at the indicated time point. **P* < 0.001, ANOVA with Dunnett's *post hoc* comparison to the wild-type control equivalent time point. *N* = 20 animals per genotype and time point. Error bars indicate SEM.

linoleic acid (ALA), but fail to produce normal amounts of other PUFAs (Fig 6A) (Watts & Browse, 2002). Taken together, our results suggest that (i) eicosanoids can play an instructive rather than a permissive role in UPS activity, as UPS activity can be driven either up or down depending on the eicosanoid profile, and (ii) the full profile of PUFAs and their derivative eicosanoids should be considered when assessing the role of lipid signaling in UPS activity.

Is increased UPS activity responsible for the reduced levels of Ub^{G76V}-GFP in *fat-1*, *fat-3*, and *fat-4* L4 + 24 h mutants? We generated lysates of L4 + 24 h and L4 + 48 h nematodes and incubated them with the fluorescent chymotryptic substrate Suc-Leu-Leu-Val-Tyr-AMC to measure epoxomicin-sensitive proteasome activity. As expected, the control *skn-1(zj15)* lysates showed reduced activity (Fig 6D). We did not observe a substantial change in proteasome activity in *fat-1* or *fat-3* mutants compared with wild type (Fig 6D). However, *fat-4* mutants showed an elevated level of proteasome activity at L4 + 24 h but a reduced level of activity at L4 + 48 h (Fig 6D), suggesting that one or more PUFAs or their eicosanoid derivatives can regulate 20S proteasome chymotrypsin-like activity.

If the elevated levels of *n*-6 eicosanoids produced in *fat-1* mutants are promoting UPS activity, then the precocious turnover of Ub^{G76V}-GFP in these mutants should depend on biogenic amine signaling, as such signaling promotes the expression of P450 enzymes like *cyp-34A4* needed to convert PUFAs into eicosanoids (Fig EV4). We examined Ub^{G76V}-GFP levels in double mutants between *fat-1* and either *tph-1* or *tdc-1*. We found that these double mutants resembled their respective *tph-1* or *tdc-1* single mutants (Fig 6E), suggesting that the augmented UPS activity observed in *fat-1* mutants requires biogenic amine signaling.

If augmented UPS activity is responsible for precocious turnover of Ub^{G76V}-GFP in mutants like *fat-1*, then a reduction in the UPS should suppress that turnover. Eggs harboring the *odIs77* transgene were hatched on bacterial lawns expressing RNAi constructs for either the UFD complex subunit *ufd-1*, the proteasome core particle subunit *pbs-5*, or an empty vector as control. As in Fig 1, we found that Ub^{G76V}-GFP levels in wild type were elevated relative to control in the *ufd-1* and *pbs-5* RNAi knockdown experiments by both day 1 (L4 + 24 h) and day 2 (L4 + 48 h) adulthood (Fig 6F). Knockdown of *pbs-5* but not *ufd-1* resulted in some stabilization of Ub^{G76V}-GFP in *fat-1* mutants at L4 + 24 h, although the reporter in these mutants was soon degraded at L4 + 48 h (Fig 6F). These results suggest that

overall UPS activity is increased in *fat-1* mutants, although as RNAi does not completely eliminate UFD complex or proteasome activity, we cannot rule out the activation of additional protein quality control mechanisms in these mutants.

One such alternative mechanism for removing ubiquitinated proteins is autophagy, and the treatment of nematodes with *n*-6 PUFAs like AA can activate autophagy (O'Rourke *et al*, 2013). We introduced the *odIs77* transgene into *lgg-1* mutants, which are impaired for autophagy (Alberti *et al*, 2010). Surprisingly, *lgg-1* mutants showed precocious turnover of Ub^{G76V}-GFP compared with wild type (Fig 6G). Mutants for *lgg-1* are sterile and must be maintained as heterozygotes, which are fertile. We noticed that *lgg-1/+* heterozygotes also showed precocious turnover of Ub^{G76V}-GFP, although not to the extent of *lgg-1* homozygotes (Fig 6G). We also examined *lgg-1 fat-1* double mutants and observed a similar precocious and elevated turnover of Ub^{G76V}-GFP (Fig 6G). Our results suggest that the *n*-6 PUFAs that accumulate in *fat-1* mutants do not promote Ub^{G76V}-GFP turnover by activating autophagy. Indeed, increased Ub^{G76V}-GFP turnover in *lgg-1* mutants suggests that UPS activity is elevated in the absence of autophagy, consistent with the compensatory upregulation of the former to offset the loss of the latter (Ji & Kwon, 2017; Nam *et al*, 2017).

Discussion

Multicellular organisms use diverse and decisive pathways, including the UPS, to regulate proteostasis in response to extrinsic and intrinsic sources of proteotoxic stress. We propose that the *C. elegans* nervous system uses biogenic amine neurotransmitters and eicosanoid signaling to regulate UPS proteostasis. Using a transgene expressing the metastable chimeric protein Ub^{G76V}-GFP, which is a UPS substrate, we examined UPS activity in mutants that fail to synthesize different biogenic amines in *C. elegans*. We found that the biogenic amine neurotransmitters DA, 5-HT, and TA promote the rapid Ub^{G76V}-GFP turnover that occurs in epithelia as nematode transition into fertile adulthood. We also found that endogenous poly-ubiquitinated proteins accumulate in mutants that fail to synthesize DA, 5-HT, or TA. Supplementation with exogenous biogenic amines can rescue their respective synthesis mutants, and supplementation of exogenous 5-HT causes precocious Ub^{G76V}-GFP

turnover to otherwise wild-type animals. We found that these biogenic amines are needed for the full expression of the CYP34 family of cytochrome P450 monooxygenases. CYP34 P450 enzymes produce eicosanoid signaling molecules from PUFAs, and we found that DA and 5-HT are required for the full expression of eicosanoids. One of these biogenic amine-regulated P450s, *cyp-34A4*, is needed for the turnover of Ub^{G76V}-GFP in adults, and *cyp-34A4* mutations block the precocious Ub^{G76V}-GFP turnover triggered by supplemental 5-HT, supporting the hypothesis that biogenic amines act through *cyp-34A4* to regulate UPS activity. P450 monooxygenases produce eicosanoids with the assistance of cytochrome P450 reductases; as expected, Ub^{G76V}-GFP turnover is impaired in mutants for the *C. elegans* reductase *emb-8*. Eicosanoids can be derived from *n*-3 or *n*-6 PUFAs, and we found that *fat-2* mutants impaired for all PUFA synthesis show impaired Ub^{G76V}-GFP turnover. By contrast, *fat-1* mutants, which synthesize *n*-6 but not *n*-3 PUFAs, trigger the opposite phenotype, precocious Ub^{G76V}-GFP turnover, suggesting that different eicosanoids have opposing roles in regulating UPS proteostasis and that eicosanoid signaling *per se* has an instructive rather than a permissive role in this regulation. Our results suggest that neurons use biogenic amine neurotransmitters as neurohormonal signals to modulate eicosanoid production from PUFAs and that these eicosanoids in turn regulate UPS proteostasis response pathways in non-neuronal tissues (Fig 7).

One of the key regulators of proteostasis in *C. elegans* is SKN-1, which has a dual function in embryonic development and in promoting the expression of xenobiotic detoxification enzymes in response to oxidative stress (An & Blackwell, 2003). The expression of proteasome subunit genes is reduced in *skn-1* mutants (Li et al, 2011; Niu et al, 2011; Keith et al, 2016). We therefore examined both Ub^{G76V}-GFP turnover and proteasome activity in *skn-1(zj15)*, a fertile hypomorphic allele, and *skn-1(tm3411)*, a null deletion allele that results in sterile animals (Ruf et al, 2013; Tang et al, 2015). Ub^{G76V}-GFP remained stable, and proteasome activity was decreased in these mutants, consistent with decreased proteasome subunit expression. SKN-1 has traditionally been considered an ortholog of human Nrf2 because of its shared role in oxidative stress response. Although Nrf2 does not appear to regulate proteasome subunit expression in mammals, closely related Nrf1 does induce proteasome expression (Radhakrishnan et al, 2010; Steffen et al, 2010; Sha & Goldberg, 2014). Thus, SKN-1 likely represents an ancestral form of these two transcription factors, mediating both of their functions. It later diverged into two factors during mammalian evolution to handle each function separately.

Ub^{G76V}-GFP levels change dramatically as animals transition into day 2 fertile adults, and multiple lines of evidence indicate that this reflects changes in UPS activity (Liu et al, 2011). The internal control mRFP is expressed from the same promoter and shares the same 5'UTR and 3'UTR regions as Ub^{G76V}-GFP. Both reporters are expressed from the same integrated transgene. The levels of Ub^{G76V}-GFP and mRFP mRNA do not change as animals enter fertile adulthood (Joshi et al, 2016). Mutating specific lysines on the Ub^{G76V}-GFP transgene prevents the decrease in Ub^{G76V}-GFP in day 2 (L4 + 48 h) adults, as does knocking down proteasome or UFD complex activity by RNAi (Liu et al, 2011). Thus, it seems unlikely that the decrease in Ub^{G76V}-GFP levels is due to decreases in reporter transcription or translation, but rather is due to changes in the ability of the UPS to recognize and degrade the reporter.

If the accumulation of Ub^{G76V}-GFP in biogenic amine signaling mutants was due to a decrease in proteasome activity, then we should have detected a healthy decrease in our direct measurement of chymotrypsin-like proteasome activity. One possibility is that biogenic amine signaling directly promotes the activity of the UFD complex rather than the proteasome. The physiological function of the UFD complex remains unclear, but it appears to act as an E4 ubiquitin ligase, recognizing proteins that have been mono- and poly-ubiquitinated by E3 ubiquitin ligases and amplifying their ubiquitin tagging through the addition of more ubiquitin moieties and the extension of the ubiquitin chain (Hoppe, 2005). Thus, the UFD complex provides an additional layer of global UPS proteostasis control, and its regulation could determine the sensitivity of a cell to general proteotoxic stressors like oxidized or unfolded proteins. Consistent with this idea, mutants for UFD complex genes show reduced lifespan and sensitivity to proteotoxic stress (Mouysset et al, 2006; Liu et al, 2011). We did not observe significant changes in the expression of UFD complex components in our analysis of biogenic amine mutants. However, it remains possible that biogenic amines promote UFD complex activity by a post-translational mechanism. We also cannot rule out the possibility that biogenic amine signaling regulates some other aspect of the 26S proteasome, including the two other 20S protease activities, substrate recognition and unfolding by the 19S subunit, the activity of proteasome-associated deubiquitinating enzymes, or the activity of substrate shuttling factors.

An alternative possibility is that biogenic amine signaling activates other proteostasis mechanisms and that the stabilization of Ub^{G76V}-GFP observed in the absence of biogenic amines is due to the UPS becoming overwhelmed handling the full proteostatic load left by the absence of these other mechanisms. In this model, proteasome activity *per se* is not disrupted in the biogenic amine signaling mutants, consistent with our direct biochemical measurements of proteasome activity with fluorescent small-molecule substrates. Rather, the ability of the proteasome to obtain access to all ubiquitinated substrates *in vivo*, including our Ub^{G76V}-GFP reporter, is disrupted. Our analysis of gene expression changes in biogenic amine mutants relative to wild type did not identify obvious alternative proteostasis pathways, but we did notice that biogenic amines were required to promote the expression of the CYP34 subfamily of P450s. The CYP34 subfamily is part of the larger CYP2 family, some members of which metabolize biogenic amine neurotransmitters, raising the possibility that the upregulation of CYP34 P450s by biogenic amines might act as a feedback, either positive or negative, to regulate biogenic amine signaling (Haduch & Daniel, 2018). Some mammalian CYP2 family members metabolize PUFAs into eicosanoids, and we observed a decrease in eicosanoid levels in *C. elegans* mutants defective for 5-HT and DA synthesis. Thus, eicosanoids might be the link between these two biogenic amines and UPS proteostasis.

Eicosanoids are produced from long-chain PUFAs. Mutants that block the synthesis of all PUFAs resulted in the stabilization of Ub^{G76V}-GFP, suggesting that one or more eicosanoid derivatives regulate UPS activity and/or proteostasis. Such mutants are a bit extreme, as the absence of all PUFAs as well as their eicosanoid derivatives could result in observed phenotypes that are due to pleiotropic effects of losing so many of these molecules, which would cast PUFAs and eicosanoids in an indirect and permissive

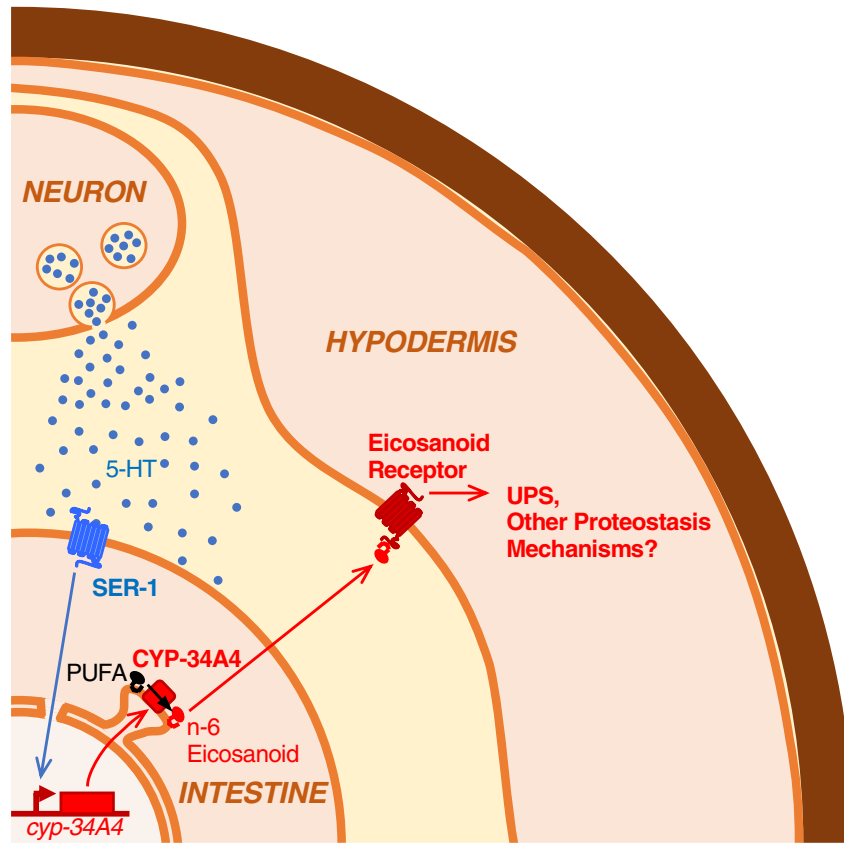


Figure 7. Working model for biogenic amine regulation of UPS proteostasis.

Cartoon cross section of nematode body showing neurons, intestine, and hypodermis. Our data suggest a model in which neurons release biogenic amines like 5-HT into the body cavity as a neurohormone. Molecules of 5-HT bind receptors like SER-1, resulting in augmented transcription of P450 enzymes like CYP-34A4. It is possible that 5-HT and other biogenic amines signal to another regulatory layer of neurons, which in turn release peptide-based signals (not shown). CYP-34A4 converts *n*-6 PUFAs into *n*-6 eicosanoids, which are released from the ER and allowed to diffuse extracellularly. Released eicosanoids could act through receptors in the hypodermis, triggering changes in UPS activity in this tissue. This triangle of signaling affords multiple points of regulation to coordinate external environment, internal physiology, and UPS proteostasis.

role in UPS proteostasis. Surprisingly, *fat-1* mutants, which fail to produce *n*-3 PUFAs but synthesize augmented levels of *n*-6 PUFAs (and presumably their eicosanoid derivatives), show precocious Ub^{G76V}-GFP turnover. This finding suggests that the specific balance of eicosanoids can either increase or decrease UPS activity and/or proteostasis, which casts PUFAs and eicosanoids in a more interesting instructive rather than permissive role in UPS proteostasis. Several *n*-6 PUFAs activate autophagy (O'Rourke *et al*, 2013), raising the possibility that Ub^{G76V}-GFP is removed by autophagy in *fat-1* mutants. However, we found that mutations in the autophagy gene *lgg-1* did not block precocious Ub^{G76V}-GFP turnover in *fat-1* mutants, ruling out this possibility. By contrast, RNAi knockdown of proteasome subunit *pbs-5* and UFD subunit *ufd-1* did reduce precocious Ub^{G76V}-GFP turnover in *fat-1* mutants, suggesting that augmented UPS activity is largely responsible.

The difference in phenotype when *n*-3 versus *n*-6 PUFA synthesis is disrupted would also suggest that different eicosanoids can have opposite effects on the same physiological process. Such disparate roles for different eicosanoids have been previously observed. For example, 20-HETE, an eicosanoid

derived from *n*-6 PUFAs, has the opposite effect on blood pressure and heart arrhythmia observed for 17,18-EEQ, an eicosanoid derived from *n*-3 PUFAs (Fleming, 2011). The best understood “classic” eicosanoids are those derived from AA and EPA, yet *fat-4* mutants, which fail to make either of these PUFAs, still show some precocious Ub^{G76V}-GFP turnover. However, eicosanoids can be derived from other PUFAs besides just AA and EPA. For example, LA-derived eicosanoids include leukotoxin and iso-leukotoxin, which inhibit mitochondrial function and can trigger apoptosis in mammals (Sakai *et al*, 1995; Stevens & Czuprynski, 1996). In *C. elegans*, eicosanoid derivatives of the PUFA DGLA induce germ cell death (Deline *et al*, 2015). Moreover, we cannot rule out that the true signaling molecules regulating UPS activity are either novel molecules derived from classic eicosanoids through additional steps beyond P450, or nonclassical eicosanoids derived from PUFAs, similar to endocannabinoids (Cascio & Marini, 2015). Assigning specific physiological functions to specific eicosanoids will require a combined biochemical and genetic analysis of different PUFA synthesis enzyme and CYP mutants.

How might an eicosanoid signal regulate UPS proteostasis? Eicosanoids bind to cell surface receptors like GPCRs and nuclear hormone receptors like PPAR (Brink, 2007; Marion-Letellier *et al*, 2016). The *C. elegans* genome contains a diverse number of GPCRs and nuclear hormone receptors to match the diverse number of CYP genes, including the CYP families that produce eicosanoids. One or more of these CYP genes might produce a specific eicosanoid that then regulates UPS proteostasis through transcriptional or post-translational means. Interestingly, *n-6* PUFAs were shown in *C. elegans* to regulate lifespan through the activation of autophagy, another proteostasis mechanism that complements the UPS (O'Rourke *et al*, 2013). Different PUFA-derived signals might directly regulate the balance between autophagy and the UPS. Alternatively, changes in the PUFA profile might alter the total proteostatic load in a cell (e.g., by altering mitochondrial function and/or oxidative stress levels), either augmenting or overwhelming UPS capacity and thereby increasing or decreasing protein turnover, respectively. Regardless of the specific mechanism, our findings raise the interesting possibility that the beneficial health effects of diets rich in fish oils, including *n-3* and *n-6* PUFAs, might be due in part to the regulation of proteostasis mechanisms like the UPS and autophagy.

Materials and Methods

Strains and growth conditions

Standard methods were used to culture *C. elegans* (Brenner, 1974). Animals were grown at 20°C on standard NGM plates seeded with OP50 *Escherichia coli* unless otherwise indicated. The following strains were provided by the *Caenorhabditis* Genetics Center: *cat-2* (*e1112*), *cat-2* (*n4547*), *cyp-34A4* (*gk933903*), *cyp-34A4* (*gk690081*), *cyp-34A4* (*gk759290*), *lgg-1* (*tm3489*), *tph-1* (*mg280*), *tdc-1* (*n3419*), *tdc-1* (*ok914*), *tbh-1* (*ok1196*), *tbh-1* (*n3243*), *fat-1* (*wa9*), *fat-2* (*ok873*), *fat-3* (*ok1126*), *fat-4* (*wa14*), *fat-7* (*wa36*), *nhr-49* (*ok2165*), *daf-16* (*mgDf50*), *hsf-1* (*sy441*), *pqm-1* (*ok485*), *skn-1* (*zj15*), and *skn-1* (*tm3411*). Transgenic strains *odIs76*[*P_{col-19}::Ub^{G76V}-GFP*, *P_{col-19}::mRFP*] and *odIs77*[*P_{col-19}::Ub^{G76V}-GFP*, *P_{col-19}::mRFP*] have been described previously (Liu *et al*, 2011). When possible, researchers were blinded to the genotype of the observed sample.

CRISPR/Cas9

CRISPR/Cas9 system was carried out using a CRISPR-Cas9-RNP injection mixture with the following final concentrations: *cyp-34A4* guide RNA (28 μM), Cas9 nuclease (2.5 μg/μl), *dpy-10* guide RNA (12 μM), *dpy-10* repair oligo (0.5 μM), trans-activating crRNA (-tracrRNA; 40 μM), KCl (25 mM), and HEPES, pH 7.4 (7.5 mM). These components were homogeneously mixed by gentle pipetting and allowed to incubate at 37°C for 15 min. After incubation, the mixture was filtered and loaded into a microinjection pipette, and the gonads of 24 adults (adulthood day 1) were injected using the standard microinjection technique. Injected P0 worms were allowed to recover at 20°C. After 3 days, 51 Rol and/or Dpy worms were picked to individual plates, allowed to produce self-progeny. Genomic DNA of the F3 generation was extracted and screened by PCR for rearrangements at the *cyp-34A4* loci. Candidate mutants were singled to NGM plates and confirmed by DNA sequencing of

genomic PCR products. All knockout mutant animals were transferred to new plates and outcrossed for at least three generations to eliminate off-targets.

Developmental timing analysis

Eggs were released from day 1 adults by alkaline bleach treatment, grown at 20°C on NGM plates seeded with OP50, then examined at specific time points for vulval morphology. Animals were deemed to have reached the L4 stage when their vulva acquired a toroidal “tree-like” structure, whereas a separate set of animals were deemed to have reached mature adulthood when their vulva acquired open and protruded morphology with a clear connection to the uterus (MacNeil *et al*, 2013). Developmental timing was modeled with a Kaplan–Meier curve, marking the time point at which each animal transitioned from pre-L4 into L4 (or pre-adult into adult). No more than 10% of animals were censored because they either died or were lost on the plate before reaching the appropriate stage of analysis.

Behavioral analysis

Synchronized L1 nematodes were grown at 20°C on NGM plates seeded with OP50, synchronized again on fresh plates at the L4 stage, then grown an additional 48 h. To quantify egg laying, the number of eggs present *in utero* was counted for each animal for each genotype, as defects in egg laying result in the accumulation of eggs *in utero*. To quantify pharyngeal pumping, 10-s movies of individual animals on plates were captured with iPhone video (Apple) using a dissection microscope and an iPhone adapter (Gskyer). Movie playback was slowed 10-fold for each animal in iMovie (Apple), allowing observers to count individual pumps. All experiments were performed in triplicate.

RNA-seq analysis

Developmentally synchronized animals were obtained by hypochlorite treatment of gravid adults to release embryos. Synchronized embryos were hatched on NGM plates and grown at 20°C until 48 h after the L4 stage of development. Fluorodeoxyuridine was used to prevent the development of second-generation embryos once animals reached fertile adulthood (Gandhi *et al*, 1980). For each RNA-seq experimental replicate, populations were grown simultaneously under the same conditions. Total RNA from several large NGM plates was isolated from animals using TRIzol (Invitrogen) combined with Bead Beater lysis in four biological replicates for each genotype. Yields ranged from 2.8 to 6.4 μg per sample. An mRNA library (single-end, 75-bp reads) was prepared for each sample/replicate using Illumina Truseq with Poly-A selection (RUCDR). Libraries were sequenced on an Illumina HiSeq 2500 in Rapid Run Mode, resulting in high-quality sequence reads (FAST QC Phred score average of 40 out to the full 75 bp length). Reads (30–40 million per genome and replicate) were mapped to the *C. elegans* genome (WS245) and gene counts generated with STAR 2.5.1a, from 93 to 95% of reads uniquely mapped to the genome. Normalization and statistical analysis on gene counts were performed with EdgeR using generalized linear model functionality and tagwise dispersion estimates. An MDS plot revealed the fourth replicate for each genotype was subject to a strong batch effect, so the fourth

replicate samples were dropped, and all analyses re-run using only replicates one, two, and three from each genotype. Likelihood ratio tests were conducted for each biogenic amine mutant relative to wild-type *odIs77* in a pairwise fashion with a Benjamini and Hochberg correction. Lists of differentially expressed genes were analyzed by DAVID (v6.8, david.abcc.ncifcrf.gov/home.jsp) using functional annotation clustering and a low classification stringency as the method for assessing annotation enrichment. List comparisons and Venn diagrams were generated using Venny (Oliveros, 2007).

RNA extraction and qRT-PCR

Synchronized animals were plated on NGM with OP50 as embryos and allowed to grow to L4 + 24 h and L4 + 48 h at 20°C. Animals were then collected in M9 buffer and washed 3× times. Approximately 200 µl of worm pellet was collected in 2-ml screw cap tubes containing 200 µl of 0.5-mm-diameter Zirconia/Silica microbeads (BioSpec Products, Cat #11079105z) and 1 ml TRIzol reagent (Ambion). Worms were flash-frozen in liquid nitrogen and stored at -80°C. For extraction, samples were allowed to thaw and were lysed using a mini-beadbeater (BioSpec), beating for 30 s, and cooling on ice for 30 s for three cycles. Lysed samples were centrifuged at maximum speed in a microcentrifuge at 4°C for 15 min. RNA was then extracted from the supernatant using the manufacturer's directions from the Direct-Zol RNA Miniprep Plus kit (Zymo Research, Cat # R2070). Final elution was in 100 µl of RNase-free water. For qRT-PCR, 50 ng of total RNA was amplified using the iTaq Universal SYBR Green One step kit (Bio-rad, Cat #1725150), and relative quantification was performed for GFP, mRFP, and actin using the primers below:

GFPqPCR-F: 5'-GGCAAGCTGACCCTGAA-3'/GFPqPCR-R: 5'-GGACTTGAAGAAGTCGTGCT-3'/mRFPqPCR-F: 5'-GACTACTTGAAGCTGTCCTTCC-3'/mRFPqPCR-R: 5'-CGCAGCTTACCTTGTAGAT-3'/ActqPCR-F: 5'-TTACTCTTTACCACCACCGCTGA-3'/ActqPCR-R: 5'-TCGTTTCCGACGGTGATGACTTGT-3'

RNAi feeding

RNAi feeding protocols were as described previously (Timmons et al, 2001). *Escherichia coli* (HT115) producing dsRNA for individual genes was seeded onto NGM plates containing 25 µg/ml carbenicillin and 0.2% lactose to induce the expression of the dsRNA for the gene of interest. The negative control was conducted by seeding the plates with HT115 containing empty vector pL4440. Synchronized embryos were hatched on each plate and grown at 20°C until 48 h after the L4 stage of development. The respective clones contained sequences for *ufd-1* or *pbs-5* in RNAi vectors and were obtained from OpenBiosystems.

Drug feeding

Synthetic DA (Sigma-Aldrich H8502) added to the NGM media of plates during their production to a final concentration of 1 mM. Synthetic 5-HT (Sigma-Aldrich H7752) was added as solution to solidified NGM agar plates and allowed to equilibrate overnight to a final concentration of 1 mM. Plates were seeded with OP50 bacteria, and approximately 20 L4 animals per genotype were

added to each plate, maintained at 20°C, and analyzed either 24 or 48 h later. No developmental delay was noticed for either drug treatment.

Epifluorescence microscopy, imaging analysis, and intensity measurements

GFP- and mRFP-tagged fluorescent proteins were visualized in nematodes by mounting on 2% agarose pads with 10 mM tetramisole. Fluorescent images of *odIs76* and *odIs77* transgenic animals were observed using an AxioImager M1m (Carl Zeiss, Thornwood, NY). A 5 × (numerical aperture 0.15) PlanApo objective was used to detect GFP and mRFP signal. Imaging was done with an ORCA charge-coupled device camera (Hamamatsu, Bridgewater, NJ) by using iVision software (BioVision Technologies, Uwhchlan, PA). Exposure times were chosen to capture at least 95% of the dynamic range of fluorescent intensity of all samples. GFP fluorescence was quantified by obtaining outlines of worms using images of the mRFP control. The mean fluorescence intensity within each outline was calculated (after subtracting away background coverslip fluorescence) for Ub^{G76V}-GFP and mRFP signals using ImageJ. The mean of raw fluorescence intensity values did not deviate more than 15% from experiment to experiment; nevertheless, individual fluorescence intensity values were normalized to the mean for control animals (wild-type *odIs77* animals at L4 + 24 h) analyzed in each experiment. Twenty animals were chosen per genotype so as to observe an effect size at least as large as the coefficient of variation. All data with normal distributions were analyzed with GraphPad Prism 8 in most cases using ANOVA with Dunnett's *post hoc* test or a Student t-test (two-tailed) with Holm-Sidak correction for multiple comparisons.

Confocal microscopy for GFP expression analysis

Fluorescent images of *cyp-34A4::gfp* transgenic animals were observed using a Chroma/89 North CrestOptics X-Light V2 spinning disk, a Chroma/89North Laser Diode Illuminator (405-nm and 470-nm lines to detect intestinal autofluorescence and GFP, respectively), and a Photometrics PRIME95BRM16C CMOS camera. Images were collected and analyzed with MetaMorph software.

Measurement of 26S proteasome activity, GFP levels, and mRFP levels in lysates

Developmentally synchronized L4 + 24 h- and L4 + 48 h-staged animals were lysed in lysis buffer (50 mM HEPES, pH 7.5, 150 mM NaCl, 5 mM EDTA, 2 mM ATP, 1 mM dithiothreitol, and protease inhibitor cocktail tablets; Roche) using Bead Beater. Lysates were transferred to microcentrifuge tubes and centrifuged at 22,000 g for 15 min at 4°C.

To measure proteasome activity, an equal amount of protein lysate (5 µg in 20 µl lysis buffer) was premixed with either 250 ng of proteasome inhibitor (epoxomicin, Boston Biochem, prepared in 50% dimethyl sulfoxide) or an equivalent volume of vehicle (50% dimethyl sulfoxide lacking the inhibitor), followed by the addition of proteasome assay buffer (200 µl; 25 mM HEPES, pH 7.5, and 0.5 mM ethylenediaminetetraacetic acid) containing a chymotryptic substrate (80 µM Suc-Leu-Leu-Val-Tyr -AMC; Boston Biochem).

Reactions were incubated at 25°C for 1 h, and fluorescence ($\lambda_{\text{ex}} = 360 \text{ nm}$; $\lambda_{\text{em}} = 465 \text{ nm}$) was detected after every 5 min using a Tecan Infinite F200 detector. Epoxomicin-sensitive activity was generated with duplicate measurements from four independent experiments, quantified, and plotted.

To measure GFP and mRFP in lysates, 5 μg of lysate in 100 μl of lysis buffer was placed in a 96-well plate, in duplicate. GFP and mRFP fluorescence was detected using a Tecan Infinite F200 detector using a filter set for either GFP ($\lambda_{\text{ex}} = 485 \text{ nm}$; $\lambda_{\text{em}} = 535 \text{ nm}$) or mRFP ($\lambda_{\text{ex}} = 590 \text{ nm}$; $\lambda_{\text{em}} = 635$). Relative fluorescence values were calculated.

Western blotting and antibodies

Nematodes were synchronized by picking to fresh plates at L4. Protein samples (30 μl) were prepared from 20 synchronized nematodes for each genotype lysed at L4 + 48 h. Equal amounts of protein samples were resolved by electrophoresis through 12% SDS–polyacrylamide gel (Bio-Rad). Western blotting was performed using mouse anti-Ub (1:2,000, Enzo), mouse anti-GFP (1:2,000, Roche), and mouse anti-actin (1:5,000, Millipore). Western blotted proteins were visualized and quantified using fluorescent-conjugated secondary antibodies from Odyssey and Licor Imaging system. Each experiment was repeated at least five times with lysates from separate nematode preparations.

Endogenous eicosanoid measurements

The eicosanoid profile was determined for wild type as well as various mutant strains, with three independent cultures per strain. Nematodes collected at L4 + 48 h were harvested as described for the RNA-seq experiments above and then prepared for LC-MS/MS analysis essentially as described previously (Kulas *et al.*, 2008). Sample aliquots were mixed with internal standard compounds, including 19-HETE (hydroxyeicosatetraenoic acid), 20-HETE, 8,9-EET (epoxyeicosatrienoic acid), 11,12-EET, 14,15-EET, 5,6-DHET (dihydroxyeicosatrienoic acid), 8,9-DHET, 11,12-DHET, 14,15-DHET, 19-HEPE (hydroxyeicosapentaenoic acid), 20-HEPE, 8,9-EEQ (epoxyeicosatetraenoic acid), 11,12-EEQ, 14,15-EEQ, 17,18-EEQ, 5,6-DiHETE (dihydroxyeicosatetraenoic acid), 8,9-DiHETE, 11,12-DiHETE, 14,15-DiHETE, and 17,18-DiHETE (Cayman Chemicals). Separate samples were either subjected to alkaline hydrolysis followed by solid-phase extraction of the metabolites to characterize total fatty acids, or they were directly subjected to solid-phase extraction to characterize free fatty acids. HPLC and MS conditions as well as the multiple reaction monitoring for the analysis of the CYP–eicosanoid profile were exactly as described previously (Arnold *et al.*, 2010).

Data availability

The datasets produced in this study are available in the following databases: RNA-Seq data: Gene Expression Omnibus GSE145255 (<https://www.ncbi.nlm.nih.gov/geo/query/acc.cgi?acc=GSE145255>).

Expanded View for this article is available online.

Acknowledgements

We thank Matthew Kiel, Tejash Shah, and Iris Tu for their technical assistance in analyzing some of the ubiquitin reporter experiments. We thank A. Fire, the *C. elegans* Genetics Center, S. Mitani, and the Japanese National Bioresource Project for reagents and strains. We thank Hazel Schubert and Daja O'Bryant for computational assistance. We thank Eunchan Park and Cathy Savage-Dunn for comments on the manuscript. The manuscript was funded by grants from the National Institutes of Health (R01 NS42023 and R01 GM101972, to CR), as well as the New Jersey Commission on Cancer Research and the Charles and Johanna Busch Fellowship (to KKJ); these agencies had no other role in the research or the manuscript.

Author contributions

KKJ designed the genetic, molecular, behavioral, and cell biological experiments under the direct supervision of CR. CR, SP, and KKJ designed the RNA-seq analysis, and SP and MV analyzed the results. CR, RM, and KKJ designed the eicosanoid biochemical analysis, and RM performed the mass spectrometry and analyzed the results. MV conducted and analyzed the qRT–PCR experiments. KKJ, TLM, and CR collected the data and analyzed the results from the remaining experiments under the direct supervision of CR. CR and KKJ wrote the manuscript.

Conflict of interest

The authors declare that they have no conflict of interest.

References

- Alberti A, Michelet X, Djeddi A, Legouis R (2010) The autophagosomal protein LGG-2 acts synergistically with LGG-1 in dauer formation and longevity in *C. elegans*. *Autophagy* 6: 622–633
- Alkema MJ, Hunter-Ensor M, Ringstad N, Horvitz HR (2005) Tyramine functions independently of octopamine in the *Caenorhabditis elegans* nervous system. *Neuron* 46: 247–260
- An JH, Blackwell TK (2003) SKN-1 links *C. elegans* mesendodermal specification to a conserved oxidative stress response. *Genes Dev* 17: 1882–1893
- Anders S, Huber W (2010) Differential expression analysis for sequence count data. *Genome Biol* 11: R106
- Arnold C, Markovic M, Blossey K, Wallukat G, Fischer R, Dechend R, Konkel A, von Schacky C, Luft FC, Muller DN *et al* (2010) Arachidonic acid-metabolizing cytochrome P450 enzymes are targets of ω -3 fatty acids. *J Biol Chem* 285: 32720–32733
- Ashrafi K, Chang FY, Watts JL, Fraser AG, Kamath RS, Ahringer J, Ruvkun G (2003) Genome-wide RNAi analysis of *Caenorhabditis elegans* fat regulatory genes. *Nature* 421: 268–272
- Balch WE, Morimoto RI, Dillin A, Kelly JW (2008) Adapting proteostasis for disease intervention. *Science* 319: 916–919
- Bard JAM, Goodall EA, Greene ER, Jonsson E, Dong KC, Martin A (2018) Structure and function of the 26S proteasome. *Annu Rev Biochem* 87: 697–724
- Barros AG, Bridi JC, de Souza BR, de Castro JC, de Lima Torres KC, Malard L, Jorio A, de Miranda DM, Ashrafi K, Romano-Silva MA (2014) Dopamine signaling regulates fat content through beta-oxidation in *Caenorhabditis elegans*. *PLoS One* 9: e85874
- Ben-Zvi A, Miller EA, Morimoto RI (2009) Collapse of proteostasis represents an early molecular event in *Caenorhabditis elegans* aging. *Proc Natl Acad Sci USA* 106: 14914–14919
- Brenner S (1974) The genetics of *C. elegans*. *Genetics* 77: 71–94

- Brink C (2007) Structural manipulation of eicosanoid receptors and cellular signaling. *ScientificWorldJournal* 7: 1285–1306
- Butt TR, Khan MI, Marsh J, Ecker DJ, Crooke ST (1988) Ubiquitin-metallothionein fusion protein expression in yeast. A genetic approach for analysis of ubiquitin functions. *J Biol Chem* 263: 16364–16371
- Capdevila JH, Falck JR, Harris RC (2000) Cytochrome P450 and arachidonic acid bioactivation. Molecular and functional properties of the arachidonate monooxygenase. *J Lipid Res* 41: 163–181
- Carre-Pierrat M, Baillie D, Johnsen R, Hyde R, Hart A, Granger L, Segalat L (2006) Characterization of the *Caenorhabditis elegans* G protein-coupled serotonin receptors. *Invert Neurosci* 6: 189–205
- Cascio MG, Marini P (2015) Biosynthesis and fate of endocannabinoids. *Handb Exp Pharmacol* 231: 39–58
- Chase DL, Koelle MR (2007) Biogenic amine neurotransmitters in *C. elegans*. *WormBook* <https://doi.org/10.1895/wormbook.1.132.1>
- Ciechanover A, Stanhill A (2014) The complexity of recognition of ubiquitinated substrates by the 26S proteasome. *Biochem Biophys Acta* 1843: 86–96
- Ciechanover A, Kwon YT (2015) Degradation of misfolded proteins in neurodegenerative diseases: therapeutic targets and strategies. *Exp Mol Med* 47: e147
- Collins GA, Goldberg AL (2017) The logic of the 26S proteasome. *Cell* 169: 792–806
- Cortes CJ, La Spada AR (2015) Autophagy in polyglutamine disease: imposing order on disorder or contributing to the chaos? *Mol Cell Neurosci* 66: 53–61
- Dantuma NP, Lindsten K, Glas R, Jellne M, Masucci MG (2000) Short-lived green fluorescent proteins for quantifying ubiquitin/proteasome-dependent proteolysis in living cells. *Nat Biotechnol* 18: 538–543
- Deline M, Keller J, Rothe M, Schunck W-H, Menzel R, Watts JL (2015) Epoxides derived from dietary dihomo-gamma-linolenic acid induce germ cell death in *C. elegans*. *Sci Rep* 5: 15417
- Denisov IG, Makris TM, Sligar SG, Schlichting I (2005) Structure and chemistry of cytochrome P450. *Chem Rev* 105: 2253–2277
- Dobin A, Davis CA, Schlesinger F, Drenkow J, Zaleski C, Jha S, Batut P, Chaisson M, Gingeras TR (2013) STAR: ultrafast universal RNA-seq aligner. *Bioinformatics* 29: 15–21
- Duerr JS, Frisby DL, Gaskin J, Duke A, Asermely K, Huddleston D, Eiden LE, Rand JB (1999) The *cat-1* gene of *Caenorhabditis elegans* encodes a vesicular monoamine transporter required for specific monoamine-dependent behaviors. *J Neurosci* 19: 72–84
- Fleming I (2011) Cytochrome P450-dependent eicosanoid production and crosstalk. *Curr Opin Lipidol* 22: 403–409
- Frederick AL, Stanwood GD (2009) Drugs, biogenic amine targets and the developing brain. *Dev Neurosci* 31: 7–22
- Gandhi S, Santelli J, Mitchell DH, Stiles JW, Sanadi DR (1980) A simple method for maintaining large, aging populations of *Caenorhabditis elegans*. *Mech Ageing Dev* 12: 137–150
- Gotoh O (1998) Divergent structures of *Caenorhabditis elegans* cytochrome P450 genes suggest the frequent loss and gain of introns during the evolution of nematodes. *Mol Biol Evol* 15: 1447–1459
- Haduch A, Daniel WA (2018) The engagement of brain cytochrome P450 in the metabolism of endogenous neuroactive substrates: a possible role in mental disorders. *Drug Metab Rev* 50: 415–429
- Hare EE, Loer CM (2004) Function and evolution of the serotonin-synthetic *bas-1* gene and other aromatic amino acid decarboxylase genes in *Caenorhabditis*. *BMC Evol Biol* 4: 24
- Hipp MS, Kasturi P, Hartl FU (2019) The proteostasis network and its decline in ageing. *Nat Rev Mol Cell Biol* 20: 421–435
- Hobson RJ, Hapiak VM, Xiao H, Buehrer KL, Komuniecki PR, Komuniecki RW (2006) SER-7, a *Caenorhabditis elegans* 5-HT7-like receptor, is essential for the 5-HT stimulation of pharyngeal pumping and egg laying. *Genetics* 172: 159–169
- Hoppe T (2005) Multiubiquitylation by E4 enzymes: 'one size' doesn't fit all. *Trends Biochem Sci* 30: 183–187
- Huang da W, Sherman BT, Lempicki RA (2009a) Bioinformatics enrichment tools: paths toward the comprehensive functional analysis of large gene lists. *Nucleic Acids Res* 37: 1–13
- Huang da W, Sherman BT, Lempicki RA (2009b) Systematic and integrative analysis of large gene lists using DAVID bioinformatics resources. *Nat Protoc* 4: 44–57
- Ji CH, Kwon YT (2017) Crosstalk and interplay between the ubiquitin-proteasome system and autophagy. *Mol Cells* 40: 441–449
- Johnson ES, Ma PC, Ota IM, Varshavsky A (1995) A proteolytic pathway that recognizes ubiquitin as a degradation signal. *J Biol Chem* 270: 17442–17456
- Joshi KK, Matlack TL, Rongo C (2016) Dopamine signaling promotes the xenobiotic stress response and protein homeostasis. *EMBO J* 35: 1885–1901
- Keith SA, Maddux SK, Zhong Y, Chinchankar MN, Ferguson AA, Ghazi A, Fisher AL (2016) Graded proteasome dysfunction in *Caenorhabditis elegans* activates an adaptive response involving the conserved SKN-1 and ELT-2 transcription factors and the autophagy-lysosome pathway. *PLoS Genet* 12: e1005823
- Kirkin V, McEwan DG, Novak I, Dikic I (2009) A role for ubiquitin in selective autophagy. *Mol Cell* 34: 259–269
- Klein MO, Battagello DS, Cardoso AR, Hauser DN, Bittencourt JC, Correa RG (2019) Dopamine: functions, signaling, and association with neurological diseases. *Cell Mol Neurobiol* 39: 31–59
- Kocaturk NM, Gozuacik D (2018) Crosstalk between mammalian autophagy and the ubiquitin-proteasome system. *Front Cell Dev Biol* 6: 128
- Kulas J, Schmidt C, Rothe M, Schunck WH, Menzel R (2008) Cytochrome P450-dependent metabolism of eicosapentaenoic acid in the nematode *Caenorhabditis elegans*. *Arch Biochem Biophys* 472: 65–75
- Li X, Matilainen O, Jin C, Glover-Cutter KM, Holmberg CI, Blackwell TK (2011) Specific SKN-1/Nrf stress responses to perturbations in translation elongation and proteasome activity. *PLoS Genet* 7: e1002119
- Lim J, Yue Z (2015) Neuronal aggregates: formation, clearance, and spreading. *Dev Cell* 32: 491–501
- Lints R, Emmons SW (1999) Patterning of dopaminergic neurotransmitter identity among *Caenorhabditis elegans* ray sensory neurons by a TGFbeta family signaling pathway and a Hox gene. *Development* 126: 5819–5831
- Liu G, Rogers J, Murphy CT, Rongo C (2011) EGF signalling activates the ubiquitin proteasome system to modulate *C. elegans* lifespan. *EMBO J* 30: 2990–3003
- Loer CM, Kenyon CJ (1993) Serotonin-deficient mutants and male mating behavior in the nematode *Caenorhabditis elegans*. *J Neurosci* 13: 5407–5417
- MacNeil LT, Watson E, Arda HE, Zhu LJ, Walhout AJ (2013) Diet-induced developmental acceleration independent of TOR and insulin in *C. elegans*. *Cell* 153: 240–252
- Marion-Letellier R, Savoye G, Ghosh S (2016) Fatty acids, eicosanoids and PPAR gamma. *Eur J Pharmacol* 785: 44–49
- McGiff JC, Quilley J (1999) 20-HETE and the kidney: resolution of old problems and new beginnings. *Am J Physiol* 277: R607–R623
- McLean KJ, Sabri M, Marshall KR, Lawson RJ, Lewis DG, Clift D, Balding PR, Dunford AJ, Warman AJ, McVey JP et al (2005) Biodiversity of cytochrome P450 redox systems. *Biochem Soc Trans* 33: 796–801

- Miwa J, Schierenberg E, Miwa S, von Ehrenstein G (1980) Genetics and mode of expression of temperature-sensitive mutations arresting embryonic development in *Caenorhabditis elegans*. *Dev Biol* 76: 160–174
- Mohammad-Zadeh LF, Moses L, Gwaltney-Brant SM (2008) Serotonin: a review. *J Vet Pharmacol Ther* 31: 187–199
- Morgese MG, Trabace L (2019) Monoaminergic system modulation in depression and Alzheimer's disease: a new standpoint? *Front Pharmacol* 10: 483
- Mouyset J, Kahler C, Hoppe T (2006) A conserved role of *Caenorhabditis elegans* CDC-48 in ER-associated protein degradation. *J Struct Biol* 156: 41–49
- Nam T, Han JH, Devkota S, Lee HW (2017) Emerging paradigm of crosstalk between autophagy and the ubiquitin-proteasome system. *Mol Cells* 40: 897–905
- Ng J, Papandreou A, Heales SJ, Kurian MA (2015) Monoamine neurotransmitter disorders—clinical advances and future perspectives. *Nat Rev Neurol* 11: 567–584
- Niu W, Lu ZJ, Zhong M, Sarov M, Murray JI, Brdlik CM, Janette J, Chen C, Alves P, Preston E et al (2011) Diverse transcription factor binding features revealed by genome-wide ChIP-seq in *C. elegans*. *Genome Res* 21: 245–254
- Noble T, Stieglitz J, Srinivasan S (2013) An integrated serotonin and octopamine neuronal circuit directs the release of an endocrine signal to control *C. elegans* body fat. *Cell Metab* 18: 672–684
- O'Brien D, van Oosten-Hawle P (2016) Regulation of cell-non-autonomous proteostasis in metazoans. *Essays Biochem* 60: 133–142
- O'Brien D, Jones LM, Good S, Miles J, Vijayabaskar MS, Aston R, Smith CE, Westhead DR, van Oosten-Hawle P (2018) A PQM-1-mediated response triggers transcellular chaperone signaling and regulates organismal proteostasis. *Cell Rep* 23: 3905–3919
- Oliveros JC (2007) Venny. An interactive tool for comparing lists with Venn's diagrams
- van Oosten-Hawle P, Morimoto RI (2014) Organismal proteostasis: role of cell-nonautonomous regulation and transcellular chaperone signaling. *Genes Dev* 28: 1533–1543
- O'Rourke EJ, Kuballa P, Xavier R, Ruvkun G (2013) Omega-6 polyunsaturated fatty acids extend life span through the activation of autophagy. *Genes Dev* 27: 429–440
- Peyou-Ndi MM, Watts JL, Browse J (2000) Identification and characterization of an animal delta(12) fatty acid desaturase gene by heterologous expression in *Saccharomyces cerevisiae*. *Arch Biochem Biophys* 376: 399–408
- Prahlad V, Cornelius T, Morimoto RI (2008) Regulation of the cellular heat shock response in *Caenorhabditis elegans* by thermosensory neurons. *Science* 320: 811–814
- Radhakrishnan SK, Lee CS, Young P, Beskow A, Chan JY, Deshaies RJ (2010) Transcription factor Nrf1 mediates the proteasome recovery pathway after proteasome inhibition in mammalian cells. *Mol Cell* 38: 17–28
- Rappleye CA, Tagawa A, Le Bot N, Ahringer J, Aroian RV (2003) Involvement of fatty acid pathways and cortical interaction of the pronuclear complex in *Caenorhabditis elegans* embryonic polarity. *BMC Dev Biol* 3: 8
- Roeder T (2005) Tyramine and octopamine: ruling behavior and metabolism. *Annu Rev Entomol* 50: 447–477
- Roman RJ (2002) P-450 metabolites of arachidonic acid in the control of cardiovascular function. *Physiol Rev* 82: 131–185
- Ruf V, Holzem C, Peyman T, Walz G, Blackwell TK, Neumann-Haefelin E (2013) TORC2 signaling antagonizes SKN-1 to induce *C. elegans* mesodermal embryonic development. *Dev Biol* 384: 214–227
- Ryno LM, Wiseman RL, Kelly JW (2013) Targeting unfolded protein response signaling pathways to ameliorate protein misfolding diseases. *Curr Opin Chem Biol* 17: 346–352
- Sakai T, Ishizaki T, Ohnishi T, Sasaki F, Ameshima S, Nakai T, Miyabo S, Matsukawa S, Hayakawa M, Ozawa T (1995) Leukotoxin, 9,10-epoxy-12-octadecenoate inhibits mitochondrial respiration of isolated perfused rat lung. *Am J Physiol* 269: L326–331
- Schoch GA, Yano JK, Wester MR, Griffin KJ, Stout CD, Johnson EF (2004) Structure of human microsomal cytochrome P450 2C8. Evidence for a peripheral fatty acid binding site. *J Biol Chem* 279: 9497–9503
- Segref A, Torres S, Hoppe T (2011) A screenable *in vivo* assay to study proteostasis networks in *Caenorhabditis elegans*. *Genetics* 187: 1235–1240
- Sha Z, Goldberg AL (2014) Proteasome-mediated processing of Nrf1 is essential for coordinate induction of all proteasome subunits and p97. *Curr Biol* 24: 1573–1583
- Shore DE, Ruvkun G (2013) A cytoprotective perspective on longevity regulation. *Trends Cell Biol* 23: 409–420
- Snaith HA, Anders A, Samejima I, Sawin KE (2010) New and old reagents for fluorescent protein tagging of microtubules in fission yeast; experimental and critical evaluation. *Methods Cell Biol* 97: 147–172
- Snapp E (2005) Design and use of fluorescent fusion proteins in cell biology. *Curr Protoc Cell Biol* 27: 21.4.1–21.4.13
- Spector AA, Kim HY (2015) Cytochrome P450 epoxygenase pathway of polyunsaturated fatty acid metabolism. *Biochem Biophys Acta* 1851: 356–365
- Srinivasan S, Sadegh L, Elle IC, Christensen AG, Faergeman NJ, Ashrafi K (2008) Serotonin regulates *C. elegans* fat and feeding through independent molecular mechanisms. *Cell Metab* 7: 533–544
- Steffen J, Seeger M, Koch A, Krüger E (2010) Proteasomal degradation is transcriptionally controlled by TCF11 via an ERAD-dependent feedback loop. *Mol Cell* 40: 147–158
- Steinbaugh MJ, Narasimhan SD, Robida-Stubbs S, Moronetti Mazzeo LE, Dreyfuss JM, Hourihan JM, Raghavan P, Operana TN, Esmailie R, Blackwell TK (2015) Lipid-mediated regulation of SKN-1/Nrf in response to germ cell absence. *Elife* 4: e07836
- Stevens PK, Czuprynski CJ (1996) *Pasteurella haemolytica* leukotoxin induces bovine leukocytes to undergo morphologic changes consistent with apoptosis *in vitro*. *Infect Immun* 64: 2687–2694
- Sulston J, Dew M, Brenner S (1975) Dopaminergic neurons in the nematode *Caenorhabditis elegans*. *J Comp Neurol* 163: 215–226
- Sun J, Singh V, Kajino-Sakamoto R, Aballay A (2011) Neuronal GPCR controls innate immunity by regulating noncanonical unfolded protein response genes *Science* 332: 729–732
- Sun J, Liu Y, Aballay A (2012) Organismal regulation of XBP-1-mediated unfolded protein response during development and immune activation. *EMBO Rep* 13: 855–860
- Sze JY, Victor M, Loer C, Shi Y, Ruvkun G (2000) Food and metabolic signalling defects in a *Caenorhabditis elegans* serotonin-synthesis mutant. *Nature* 403: 560–564
- Tang L, Dodd W, Choe K (2015) Isolation of a hypomorphic *skn-1* allele that does not require a balancer for maintenance. *G3: Genes - Genomes - Genetics* 6: 551–558
- Tatum MC, Ooi FK, Chikka MR, Chauve L, Martinez-Velazquez LA, Steinbusch HW, Morimoto RI, Prahlad V (2015) Neuronal serotonin release triggers the heat shock response in *C. elegans* in the absence of temperature increase. *Curr Biol* 25: 163–174
- Taubert S, Van Gilst MR, Hansen M, Yamamoto KR (2006) A mediator subunit, MDT-15, integrates regulation of fatty acid metabolism by NHR-

- 49-dependent and -independent pathways in *C. elegans*. *Genes Dev* 20: 1137–1149
- Thompson O, Edgley M, Strasbourger P, Flibotte S, Ewing B, Adair R, Au V, Chaudhry I, Fernando L, Hutter H et al (2013) The million mutation project: a new approach to genetics in *Caenorhabditis elegans*. *Genome Res* 23: 1749–1762
- Timmons L, Court DL, Fire A (2001) Ingestion of bacterially expressed dsRNAs can produce specific and potent genetic interference in *Caenorhabditis elegans*. *Gene* 263: 103–112
- Van Gilst MR, Hadjivassiliou H, Jolly A, Yamamoto KR (2005) Nuclear hormone receptor NHR-49 controls fat consumption and fatty acid composition in *C. elegans*. *PLoS Biol* 3: e53
- Vilchez D, Morante I, Liu Z, Douglas PM, Merkwirth C, Rodrigues AP, Manning G, Dillin A (2012) RPN-6 determines *C. elegans* longevity under proteotoxic stress conditions. *Nature* 489: 263–268
- Vrablik TL, Watts JL (2013) Polyunsaturated fatty acid derived signaling in reproduction and development: insights from *Caenorhabditis elegans* and *Drosophila melanogaster*. *Mol Reprod Dev* 80: 244–259
- Wallis JG, Watts JL, Browse J (2002) Polyunsaturated fatty acid synthesis: what will they think of next? *Trends Biochem Sci* 27: 467
- Warnatsch A, Bergann T, Kruger E (2013) Oxidation matters: the ubiquitin proteasome system connects innate immune mechanisms with MHC class I antigen presentation. *Mol Immunol* 55: 106–109
- Watts JL, Browse J (2002) Genetic dissection of polyunsaturated fatty acid synthesis in *Caenorhabditis elegans*. *Proc Natl Acad Sci USA* 99: 5854–5859
- Watts JL, Browse J (2006) Dietary manipulation implicates lipid signaling in the regulation of germ cell maintenance in *C. elegans*. *Dev Biol* 292: 381–392
- Williams PA, Cosme J, Sridhar V, Johnson EF, McRee DE (2000) Mammalian microsomal cytochrome P450 monooxygenase: structural adaptations for membrane binding and functional diversity. *Mol Cell* 5: 121–131
- Yanushevich YG, Staroverov DB, Savitsky AP, Fradkov AF, Gurskaya NG, Bulina ME, Lukyanov KA, Lukyanov SA (2002) A strategy for the generation of non-aggregating mutants of Anthozoa fluorescent proteins. *FEBS Lett* 511: 11–14
- Yemini E, Jucikas T, Grundy LJ, Brown AE, Schafer WR (2013) A database of *Caenorhabditis elegans* behavioral phenotypes. *Nat Methods* 10: 877–879
- Ying L, Zhu H (2016) Current advances in the functional studies of fatty acids and fatty acid-derived lipids in *C. elegans*. *Worm* 5: e1184814
- Zeldin DC (2001) Epoxygenase pathways of arachidonic acid metabolism. *J Biol Chem* 276: 36059–36062
- Zeng C, Zhang M, Asico LD, Eisner GM, Jose PA (2007) The dopaminergic system in hypertension. *Clin Sci (Lond)* 112: 583–597
- Zheng N, Shabek N (2017) Ubiquitin ligases: structure, function, and regulation. *Annu Rev Biochem* 86: 129–157